



Deposited via The University of Sheffield.

White Rose Research Online URL for this paper:

<https://eprints.whiterose.ac.uk/id/eprint/156296/>

Version: Accepted Version

Article:

Kenney, L.P., Heller, B.W., Barker, A.T. et al. (2016) A review of the design and clinical evaluation of the ShefStim array-based functional electrical stimulation system. *Medical Engineering and Physics*, 38 (11). pp. 1159-1165. ISSN: 1350-4533

<https://doi.org/10.1016/j.medengphy.2016.08.005>

Article available under the terms of the CC-BY-NC-ND licence
(<https://creativecommons.org/licenses/by-nc-nd/4.0/>).

Reuse

This article is distributed under the terms of the Creative Commons Attribution-NonCommercial-NoDerivs (CC BY-NC-ND) licence. This licence only allows you to download this work and share it with others as long as you credit the authors, but you can't change the article in any way or use it commercially. More information and the full terms of the licence here: <https://creativecommons.org/licenses/>

Takedown

If you consider content in White Rose Research Online to be in breach of UK law, please notify us by emailing eprints@whiterose.ac.uk including the URL of the record and the reason for the withdrawal request.

1 A review of the design and clinical evaluation of the ShefStim array-based
2 functional electrical stimulation system.

3 Laurence P. Kenney*¹, Ben W. Heller², Anthony T. Barker³, Mark L. Reeves³, Jamie Healey³, Timothy R.
4 Good³, Glen Cooper^{1,4}, Ning Sha¹, Sarah Prenton^{1,5}, Anmin Liu¹, David Howard¹

5 ¹Centre for Health Sciences Research, University of Salford, Salford M6 6PU, U.K.

6 ²Centre for Sports Engineering Research, Sheffield Hallam University, Sheffield S1 1WB, U.K.

7 ³Department of Medical Physics and Clinical Engineering, Royal Hallamshire Hospital, Sheffield S10 2JF U.K.

8 ⁴School of Mechanical, Aerospace and Civil Engineering, University of Manchester, Manchester, M13 9PL,
9 U.K.

10 ⁵Division of Health and Rehabilitation, University of Huddersfield, Huddersfield HD1 3DH, U.K.

11
12 * Corresponding author: email - l.p.j.kenney@salford.ac.uk; tel 0161295 2289

13 **Abstract:** Functional electrical stimulation has been shown to be a safe and effective means of correcting foot
14 drop of central neurological origin. Current surface-based devices typically consist of a single channel
15 stimulator, a sensor for determining gait phase and a cuff, within which is housed the anode and cathode. The
16 cuff-mounted electrode design reduces the likelihood of large errors in electrode placement, but the user is still
17 fully responsible for selecting the correct stimulation level each time the system is donned. Researchers have
18 investigated different approaches to automating aspects of setup and/or use, including recent promising work
19 based on iterative learning techniques. This paper reports on the design and clinical evaluation of an electrode
20 array-based FES system for the correction of drop foot, ShefStim. The paper reviews the design process from
21 proof of concept lab-based study, through modelling of the array geometry and interface layer to array search
22 algorithm development. Finally, the paper summarises two clinical studies involving patients with drop foot.
23 The results suggest that the ShefStim system with automated setup produces results which are comparable with
24 clinician setup of conventional systems. Further, the final study demonstrated that patients can use the system
25 without clinical supervision. When used unsupervised, setup time was 14 minutes (9 minutes for automated
26 search plus 5 minutes for donning the equipment), although this figure could be reduced significantly with
27 relatively minor changes to the design.

28
29 1. INTRODUCTION

30 Functional electrical stimulation has been shown to be a safe and effective means of correcting foot drop of
31 central neurological origin [1-3]. Surface-based devices typically stimulate via a cathode placed over the
32 common peroneal nerve immediately distal to where it bifurcates into the deep and superficial branches, and an
33 anode placed over tibialis anterior. Appropriate levels of stimulation delivered via accurately placed electrodes
34 should result in suitably weighted recruitment of the two nerve branches, leading to a useful and safe foot
35 response during the swing phase of walking (dorsiflexion with a small degree of eversion). However, in certain
36 individuals even very small electrode positioning errors can lead to a poor foot response. Indeed, a 1999 survey
37 of users of drop foot stimulators reported over 40% of respondents finding electrode positioning problematic
38 [4]. Some current systems such as the WalkAide (Innovative Neurotronics Inc., Austin, Texas, USA) embed
39 electrodes in a cuff, worn below the knee (the reader is referred to [5] for a recent review of current systems).
40 Such an approach greatly reduces the likelihood of large errors in electrode placement, but the user is still fully
41 responsible for selecting the correct stimulation level each time the system is donned. Interestingly, despite
42 improvements in both stimulator designs and patient education, two recent studies demonstrated that when
43 patients set up their stimulators without clinician support, the resultant foot response is often less than optimal[6,
44 7].

45 One approach to the challenge of stimulator setup is to implant the electrodes on the nerve(s), thereby removing
46 the electrode placement problem from the user [8, 9]. However, an invasive approach carries risks and the
47 implantable devices and surgical costs remain relatively expensive. As a result, a number of groups have been
48 investigating the possibility of automating the surface-based drop foot setup process through a two-channel
49 stimulation approach to software steering of the foot [10-12], or electrode array-based approaches [13-18]. Both
50 approaches feature a 'setup space' which can be automatically searched, either through replacing single
51 electrode(s) with one or two arrays of discrete electrodes, or by allowing modulation of pulse waveform. Both

52 approaches also use measurement of foot orientation, usually derived from foot-worn inertial sensors, to guide
53 the search.

54 Elsaify proposed an automatic array element search algorithm, but using array elements with separate gel layers
55 (a matrix of small single electrodes) [14]. More recently, Valtin [17] demonstrated an array search algorithm
56 that takes roughly two minutes using two flexible PCB electrode arrays (one over the nerve and one over
57 Tibialis Anterior), each interfaced with a continuous, high-resistivity hydrogel layer. However, in contrast to the
58 work presented here, only preliminary results with a healthy subject were presented. In the most recent work,
59 Seel reported on a system using a foot-mounted inertial sensor to adjust the steering based on realtime
60 measurements of the foot orientation[11]. The system uses only two electrodes and, in laboratory studies with
61 stroke participants, demonstrates convergence on a suitable foot response within one or two strides. However,
62 studies of the system outside of the laboratory setting have yet to be published.

63 In this paper we expand on a recent conference paper [19] to report on the design, development and
64 demonstration of a system for automated setup of drop foot FES (ShefStim). The paper extends the conference
65 paper by presenting the model used to define the initial electrode array geometry design (section 2) and provides
66 discussion of the merits and limitations of ShefStim compared with alternative systems. The ShefStim design
67 concept was proposed by Heller in 2003 [20]. For this study the Department of Medical Physics at Sheffield
68 Teaching Hospitals initially developed a ‘proof-of-concept’ multi-electrode stimulator, which could
69 simultaneously stimulate any manually-selected subset out of a conveniently sized, 8 by 8 rectangular array of
70 metal electrodes. The subset of activated electrodes is termed a virtual electrode (VE). In order to develop this
71 concept into a clinically usable system for automated setup a series of design problems needed to be solved. The
72 first problem was the electrode array design; the second problem was the development of an array search
73 algorithm. The remaining part of the paper summarises the results from two studies of the ShefStim involving
74 people with drop foot of central neurological origin.

75

76 2. DESIGN OF THE ELECTRODE ARRAY

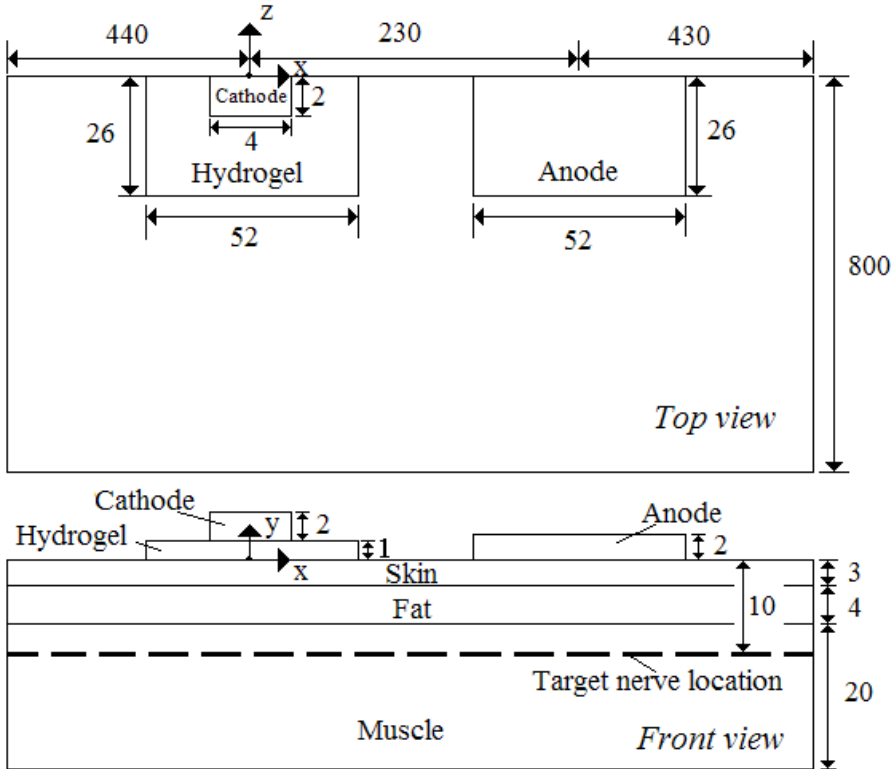
77 For clinical applications a moderately electrically conductive hydrogel interface between the electrodes and skin
78 provides the benefits of hydration of, and adhesion to, the skin. However, in array applications a continuous
79 hydrogel layer also introduces the issue of spatial selectivity loss due to transverse currents in the hydrogel.
80 Spatial selectivity is defined as the ability to activate discrete groups of nerve fibres in a localised region without
81 stimulating nerve fibres in neighbouring regions.

82 In order to achieve a satisfactory degree of spatial selectivity, it was necessary to identify an appropriate
83 electrode geometry and interface layer properties. Two finite-element models were therefore developed to
84 investigate the effects of electrode geometry and hydrogel layer properties on spatial selectivity, characterised in
85 our model by the activation area (see below). Model 1 was developed to explore the effects of hydrogel
86 resistivity and electrode size on activation area under a single cathode electrode and; Model 2 extended Model 1
87 through the addition of electrodes surrounding the cathode, to allow investigation of activation area under a
88 multi-electrode array. The results of the second model, together with practical constraints imposed by the
89 stimulator, led to the array geometry and interface layer properties used in part 3 of this paper.

90 *Model 1*

91 Figure 1 shows the 3D finite-element model, developed using ANSYS Multiphysics (Version 10.0, Ansys, Inc,
 92 Canonsburg, PA, USA) to predict the effects of electrode geometry and hydrogel properties on electric field
 93 distribution in the underlying tissue [21]. The model represents a cathode, an anode, a hydrogel layer, skin, fat
 94 and muscle. The skin, fat and muscle were modelled as flat, extended layers, whose thicknesses were based on
 95 their anatomical dimensions. As bone has much higher resistivity than the other media, it was assumed to be
 96 non-conductive volume underlying the muscle, and hence was represented as the lower boundary of the model.
 97 Structures of smaller dimension, such as hair follicles or blood vessels, were not explicitly modelled, as their
 98 influence on stimulation at the depth of the motor nerve branches could be considered negligible.

99 Appropriate electrical conductivity properties were assigned to the elements, based on values from Duck [22]
 100 (Table 1). Although the skin's capacitance cannot normally be neglected, the skin in the model was assumed to
 101 be hydrated due to intimate contact with the hydrogel layer. Hence capacitive effects were not included in this
 102 model.



103
 104 Figure 1: Schematic of the geometry of the selectivity FE model (not to scale) (dimensions in mm)

105

106 Table 1: Model parameters

Biological tissues and materials	Resistivity (Ωm)
Bone	7×10^4
Muscle	2 in X and Z directions
	4 in Y direction
Fat	62.5
Skin (hydrated)	833
Hydrogel	Model variable
Cathode and Anode	1.5×10^{-8}

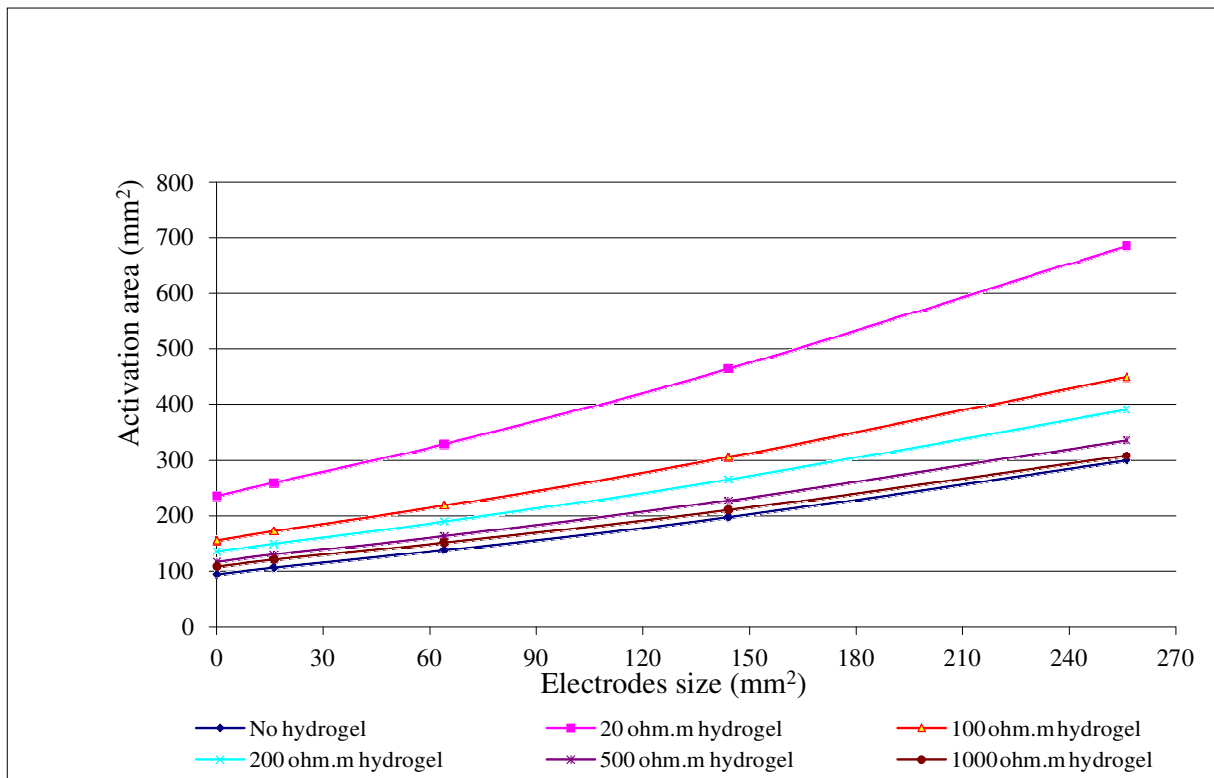
107

108 The calculation of whether a point in the model was deemed to be stimulated was based on the stimulation
 109 function [23]. To explore spatial selectivity we first defined a stimulus pool to be a volume over which the value
 110 of the stimulation function exceeds a threshold at which action potentials in a nerve fibre are generated. The
 111 maximum stimulation function always appears in the stimulus pool centre, just underneath the cathode, and the

112 amplitude of the stimulation function decreases from the centre to the edge of the stimulus pool. Although the
 113 value of the maximum stimulation function varies between models, it can always be scaled to the same value by
 114 changing the input current, and this scaling does not change the shape or size of the stimulus pool. Contours
 115 may be defined which connect points in the model with identical stimulation function values (expressed as a
 116 percentage of the maximum) and the 50% contour was selected to represent the boundary of the stimulus pool
 117 for the results presented here. The 50% contour choice was somewhat arbitrary, but avoided problems which
 118 would be associated with choice of a contour near 100% or 0% of maximum stimulation function (all contours
 119 converge to a point at 100% of maximum stimulation function and contours enclose infinitely large areas at 0%)
 120 As the electrical properties of the tissue were uniform, the current density distribution was symmetric along the
 121 plane normal to the skin surface and along the centres of the cathode and the anode. This symmetry allowed a
 122 study to be performed on a half model. To represent the location of the nerve, we defined a plane representing
 123 the anatomical depth of the target nerve (10mm). The intersection of the stimulus pool with the plane defined an
 124 area; the smaller the area, the more focused is the stimulation and thus the better the spatial selectivity.
 125 Therefore, the area of the stimulus contour associated with 50% of maximal stimulation was used as the metric
 126 of spatial selectivity.

127 To explore the combined effect of hydrogel resistivity and electrode size on selectivity, a series of simulations
 128 were run with square electrodes from infinitely small (a point) to 16mm×16mm with a range of interface layers.
 129 The first simulation considered the no interface layer case; subsequent simulations varied the 1mm thick
 130 hydrogel layer resistivity from 20Ωm to 1000Ωm. The results are shown in Figure 1.

131



132

133 *Figure 2: The effects of electrode size on activation area for a range of hydrogel resistivities.*

134

135

136 Figure 1 shows that there is a minimum limit to activation area of approximately 100mm² at 10mm depth, and
 137 that spatial selectivity becomes poorer (activation area increases) with increasing size of electrode and
 138 decreasing resistivity. When the resistivity reaches 500Ωm or greater, the spatial selectivity is similar to that
 139 of the model without the hydrogel sheet.

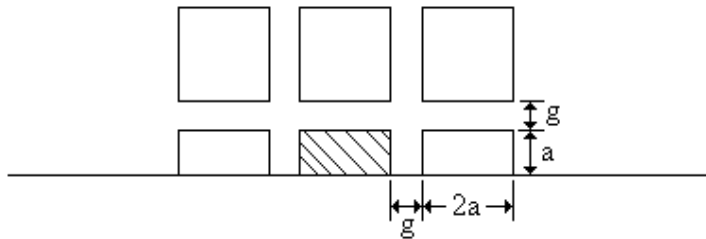
140 *Model 2*

141 Model 1 had shown that the introduction of a 1 mm hydrogel interface layer did not significantly degrade
 142 selectivity providing the hydrogel resistivity was at least 500Ωm. However, the model did not account for the
 143 presence of neighbouring electrodes which would surround an electrode in the array. The presence of these
 144 electrodes will lead to a decrease in selectivity compared with the single electrode condition, as current can flow
 145 from activated electrodes across inter-electrode gaps and into adjacent non-activated electrodes. These effects
 146 would be modulated by the size of the inter-electrode gap and hydrogel properties. Therefore, Model 1 was used
 147 as the basis for a new model (Model 2) to enable the electrode array design to be finalised.

148 It was assumed that the magnitude of reduction in selectivity due to current passing across the inter-electrode
 149 gaps would be dominated by electrodes immediately surrounding any given electrode in the array. Hence,
 150 Model 1 was extended to include eight more electrodes surrounding the original cathode electrode (Figure 2)¹.
 151 The interface between the electrode array and the skin was a sheet of hydrogel. The initial geometry of Model 2
 152 was informed by previous pilot experimental work carried out as part of a Master's research project,
 153 demonstrating the viability of using a 70mm x70mm electrode array consisting of 64 electrodes (arranged in an
 154 8x8 format)[24].

155

156



157 surrounding electrodes the stimulating electrode

158 *Figure 3: Model 2. The electrode gap (g) is the edge-to-edge distance between any two neighbouring electrodes in the*
 159 *array; 2a is the dimension of each square electrode*

160 As the feasibility work suggested maintaining an overall array size of approximately 70mm x 70mm, we fixed
 161 the centre-to-centre spacing of electrodes in the model to be 9mm ($2a + g = 9$, see Figure 2). Five different gap
 162 sizes were modelled (Table 1) and for each of these, four commercial hydrogel sheets were modelled (Table 2).
 163 The set of hydrogel properties were informed not only by the results of Model 1, but also by earlier
 164 experimental work [25, 26] which provided further evidence to support the use of a thin, high-resistivity
 165 hydrogel layer between the electrode and skin.

166 *Table 2: Electrode gap and size evaluated in the FE model, and resultant overall electrode array size*

Electrode gap (mm)	Electrode size (mm)	Electrode array size (mm)
1	8x8	71x71
2	7x7	70x70
3	6x6	69x69
4	5x5	68x68
5	4x4	67x67

167

168 *Table 3: Hydrogel materials represented in the model. Note that the different sheet thicknesses modelled were chosen to*
 169 *represent the sheet thicknesses provided by the manufacturers.*

Hydrogel (abbreviation)	Approx thickness (mm)	Resistivity at 1.67kHz (Ωm)

¹ Note, as per Model 1, a half model was developed to take advantage of symmetry.

AG703, Axelgaard manufacture Co., Ltd. Fallbrook, CA. USA (Hydrogel 703)	0.9	55
AG803, Axelgaard manufacture Co., Ltd. Fallbrook, CA. USA (Hydrogel 803)	0.9	206
SRBZAB-05SB, Sekisui Plastics, Co., Ltd. Tokyo, Japan (Hydrogel ST)	0.5	1363
AG, AG3AM03M-P10W05, Sekisui Plastics, Co., Ltd. Tokyo, Japan (Hydrogel AG)	0.3	25185

170

171

172

173

174

In order to quantify the effects of the surrounding electrodes on selectivity, two versions of each model were run. In the first version, the surrounding electrodes were not represented and in the second, the surrounding electrodes were represented. The selectivity loss resulting from the introduction of surrounding electrodes was quantified by a selectivity loss ratio, defined in equation 1.

175

$$Selectivity_loss_ratio = \frac{A_2 - A_1}{A_1} \times 100\% \quad (1)$$

176

177

178

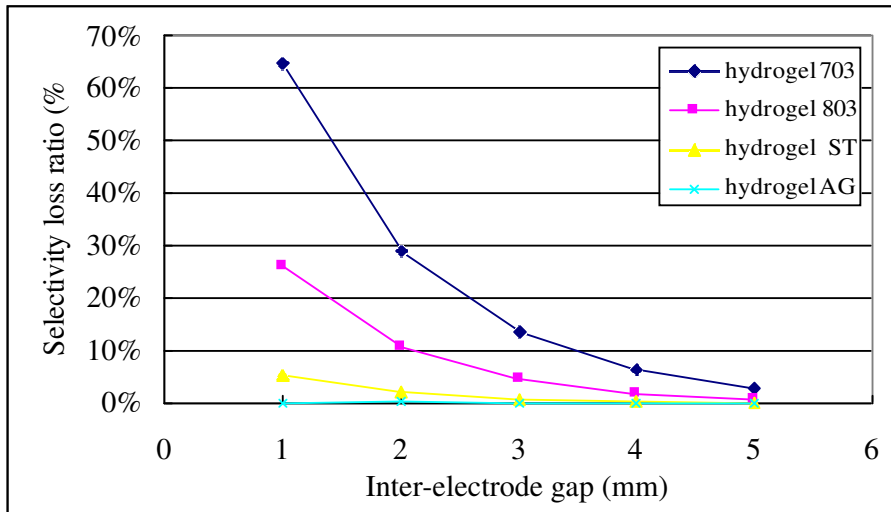
Where, A_1 is the activation area of the model without surrounding electrode and A_2 is the activation area of the model with surrounding electrode

179

180

181

Figure 3 shows the selectivity loss ratio due to the surrounding electrodes calculated for each combination of hydrogel interface layer and inter-electrode gap.



182

183

Figure 3: Selectivity loss ratios with different hydrogels

184

185

186

187

188

189

The results suggested that for hydrogels ST and AG an electrode gap between 1mm and 5mm will result in an acceptably low selectivity loss (defined as less than 10%) in the presence of the surrounding electrodes. From a manufacturing perspective, an inter-electrode gap of less than 2mm would make it very difficult to route the tracks between electrodes, so a 2mm inter-electrode gap was chosen. A final practical test demonstrated that our stimulator (200V drive voltage) could not drive the specified 8mA per channel when using the more resistive of the two most promising materials (hydrogel AG) and hence hydrogel ST was selected.

190

3. FEASIBILITY STUDY OF ELECTRODE ARRAY SEARCH STRATEGY

191

192

193

Section 3 described the design of an 8 x 8 electrode array interfaced to the skin via a thin high-resistivity hydrogel layer. The next design problem was the development of a quick, reliable method of searching the set of all possible stimulation electrodes to find the optimal virtual electrode. In this section we report on two

194 methods for searching the array used to identify appropriate virtual electrodes and their associated stimulation
195 levels, which extended the work of Elsaify et al. [14]. In the first part of the work, we apply a slowly ramped
196 stimulation through each virtual electrode while continuously monitoring the orientation of the foot relative to
197 the leg. These data allow identification of electrode sets that, when appropriately stimulated, result in acceptable
198 foot movement. The ramped stimulation results were used to investigate whether it is possible to reduce the
199 search space through prediction of the location of the best subset of these electrodes based only on the response
200 of the foot to short bursts of stimulation (twitch stimulation). We investigated use of a cost function to rank the
201 response to short bursts of stimulation and examine whether this ranking may be used to isolate smaller groups
202 of electrodes that contain one or all of the best subset of electrodes identified in the slow ramped stimulation
203 search.

204 For brevity, here we only report on the search for appropriate single VEs. Additional work to identify suitable
205 pairs of VEs is reported elsewhere [27]. Ethical approval for the study was granted by the University of
206 Salford's Research Governance and Ethics committee (RGE06/102). Twelve healthy subjects were recruited
207 from within the University and a full set of results were obtained for ten (9 male) subjects (median 30 years)².

208 The stimulation system consisted of a constant current portable 64 channel stimulator designed and built by the
209 Medical Engineering section of Sheffield Teaching Hospitals NHS Foundation Trust (size: 155 mm × 95 mm ×
210 33 mm), an 8×8 electrode array, described in section 2 and a 50×50 mm square conventional hydrogel electrode
211 (PALS® Platinum electrode, Axelgaard Manufacturing Co. Ltd.), The charge-balanced asymmetrical biphasic
212 stimulus pulses were software controllable via a graphical user interface, with the pulse width fixed at 300 μs,
213 and the frequency at 35 Hz. Stimulation intensity through each electrode was software controlled and measured
214 by an analogue to digital converter built-in to the stimulator itself. During the experiment, groups of 2×2
215 electrodes were activated simultaneously (the minimum number required to elicit adequate contractions,
216 providing a total current of up to 32 mA), and act as a virtual electrode.

217
218 A 5-camera Qualisys motion capture system (Proreflex, Qualisys AB, Sweden) was used to record foot
219 movement at 100Hz and the motion data were transferred to and simultaneously analysed in Visual3D
220 (Visual3D™, C-Motion Inc, USA). Hence the foot movement was captured, and ankle angles in sagittal,
221 coronal and transverse planes were displayed in real-time. Synchronisation between the stimulator and the
222 motion capture system was achieved using a data acquisition device via the stimulator control program. An
223 electrically-isolated button was included to allow the user to stop stimulation at any stage in the experiment.

224 The experiment started with measurement of the neutral foot orientation for the subject while standing upright.
225 He/she was then asked to sit in a chair and their right lower leg was strapped in the brackets to keep the shank in
226 a consistent pose throughout. The stimulator and electrodes were then donned. The subject was then asked to
227 maintain their sitting posture and relax the foot in a natural (dropped) position throughout the experiments. As
228 the analysis of data did not dictate the order in which the tests were conducted, the foot twitch experiment was
229 conducted first to reduce fatigue. However, here they are explained in reverse order for clarity.

230 Prior to beginning the slow ramped stimulation experiment a user-defined maximal current was identified. We
231 assumed that sensation would be most acute over bony prominences and hence at the start of the experiment
232 increased stimulation over these sites until a user-defined maximum was reached and the value noted. Next,
233 current through each VE in turn was ramped from zero to the user-defined maximal current over 10 seconds.
234 The twitch stimulation part of the experiment involved six different bursts of stimulation (1 and 4 pulses/burst,
235 at 3 different levels of stimulation (16, 24 and 32mA) being applied in turn through each of the 49 VEs. Ankle
236 angles together with time-synchronised current data for each of the different electrodes were recorded for both
237 experiments.
238

239 The target for foot orientation was defined as dorsiflexion at or above neutral, and inversion/eversion within -
240 1SD of the previously reported healthy subject mean foot orientation at heel strike [28]. All VEs which, when
241 stimulated over the 10 second period, resulted in the foot reaching the target foot orientation were identified and
242 the set of electrodes satisfying these criteria were labelled Set A.
243

244 When sitting relaxed in the chair the subject's foot was typically plantarflexed and inverted, compared with its
245 neutral position. Hence, it was assumed that a twitch response that moved the foot towards dorsiflexion and
246 eversion was desirable. A cost function was defined which used the maximum value of dorsiflexion and
247 inversion angles observed during the twitch response
248

² Two subjects could only tolerate 12.8 mA and 16 mA respectively, which was insufficient to produce target dorsiflexion when applied through any of the virtual electrodes during the slowly ramped stimulation

249 $Cost = -2 \cdot Dorsi + Inver$

250 Where *Dorsi* is the peak dorsiflexion angle (in degrees) measured during stimulation relative to the relaxed
 251 position. Dorsiflexion is positive and plantarflexion is negative. *Inver* is the peak inversion angle (in degrees)
 252 measured during stimulation relative to the relaxed position. Inversion is positive and eversion is negative. A
 253 weighting factor of 2 was applied to the dorsiflexion angle to reflect its relative importance compared to
 254 inversion/eversion.
 255

256 This cost function was used to rank the foot responses to each of the different twitch stimulation bursts applied
 257 to each of the VEs. The cost function, which was applied to the positive peak value of dorsiflexion and
 258 inversion, maximizes dorsiflexion and minimizes inversion. The VE with the lowest cost was ranked 1st and
 259 each of the remaining 48 VEs were then assigned a rank based on their cost. To identify how well the cost
 260 function could be used to predict membership of Set A (the set of VEs which, when stimulated resulted in the
 261 foot reaching the target foot orientation) two metrics were derived. First, how far down the ranking it was
 262 necessary to go to include all of the members of Set A, defined as Rank_all ; second, how far down the ranking
 263 it was necessary to go to include any member of Set A, defined as Rank_any.
 264

265 In 9 out of the 10 subjects to complete the slow ramped stimulation study, at least 1 VE was identified which,
 266 when stimulated, produced the target foot response. The maximum number of acceptable VEs found for any
 267 individual subject was 4 (out of 49) and the minimum was 0.

268 The results of the twitch stimulation analysis for the 9 subjects are shown in Table 4. Note that stimulation at
 269 16mA produced no or minimal response.

270

271 *Table 4: Rank_any and Rank_all for different twitch stimuli*

	1 pulse @ 32mA	4 pulses @32mA	1 pulse @ 24mA	4 pulses @ 24mA
Rank_all				
Median (range)	5 (1-33)	4 (1-41)	11 (2-40)	8 (2-41)
Rank_any				
Median (range)	2 (1-19)	3 (1-15)	6 (1-15)	4 (1-29)

272

273 Although there was significant inter-subject variability, the results showed that in most cases by using a cost
 274 function to rank responses to twitch stimulation it was possible to identify a much smaller set of electrodes
 275 containing one, or all of Set A. For example, using a 4 pulse burst of stimulation at 32mA, a suitable electrode
 276 was identified in all cases within the first 15 of the responses ranked according to the slow ramped stimulation
 277 results. The data suggested therefore there could be advantage to using a twitch stimulation consisting of
 278 multiple pulses at high currents and a two stage search strategy was worth further investigation.

279 **4. FIRST LAB-BASED DEMONSTRATION OF SHEFSTIM**

280 Further development work on both the stimulator and the search algorithm was carried out over the period 2009-
 281 11 resulting in the first demonstration of an array-based FES system with automated setup for the correction of
 282 drop foot. The study is reported in detail elsewhere [6], so in this paper, we focus on the improvements made to
 283 the stimulator hardware and implementation of the search algorithm, and provide an overview of the laboratory-
 284 based study involving subjects with drop foot.

285 **4.1 Stimulator**

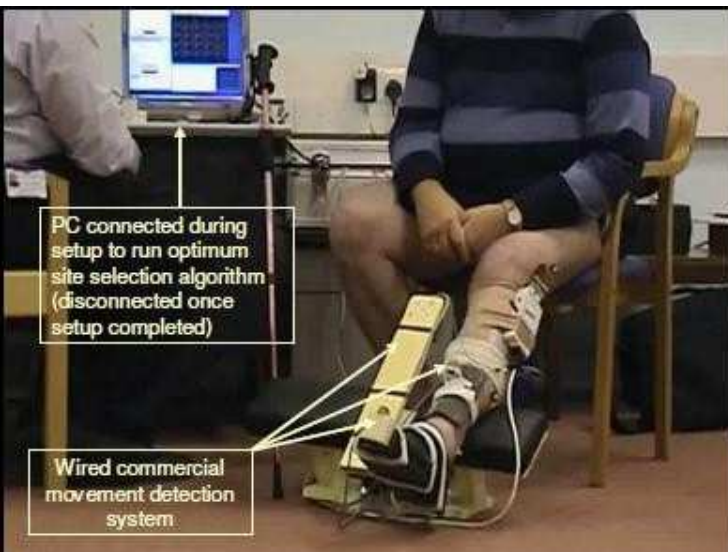
286 Further stimulator development led to a new design weighing 200 g with a volume of 211cc (130 mm x 65 mm
 287 x 25 mm). During automated setup the stimulator was controlled via an isolated serial link by a program
 288 running on an external computer, the participant's leg was held in a brace, with the knee extended and foot
 289 movement was measured using an electromagnetic position and orientation sensor (Patriot, Polhemus Inc,

290 Vermont) (Figure 4). For walking trials the setup parameters were downloaded and the stimulator disconnected
291 from the computer, enabling it to function as a standalone drop foot stimulator being triggered using a foot
292 switch.

293 4.2 Search algorithm

294 The work described in section 4 had been based on the use of a 2 x 2 VE. Following further pilot work it was
295 found that a 4 x 4 VE still provided satisfactory resolution over foot response, but reduced sensation compared
296 to a 2x2 arrangement and increased robustness to tissue movement during gait. The move to a 4 x 4 VE also
297 served to reduce the array search space by a factor of ~2, compared with the original approach (25 VEs to be
298 searched rather than 49).

299 As described in section 4, we had already demonstrated the potential to use the response of the foot to short
300 bursts of stimulation as a means of homing in on promising VEs. However, further work was needed to develop
301 a clinically usable search algorithm. In the final system a three phase search strategy was implemented.



302
303

Figure 4: Setup of ShefStim

304 In phase one the level of stimulation at which the foot first responds is determined. Short bursts of stimulation
305 are applied to each of the 25 virtual electrodes, a process taking about 2.5 seconds. The amplitude is
306 automatically titrated until the threshold for repeatable foot movement, irrespective of direction, is determined.
307 This threshold amplitude is used as the base for searches in subsequent phases. In phase two (twitch response),
308 the algorithm searches for candidate stimulation sites, using twitches rather than tetanic contractions to speed-up
309 search time and reduce sensation. Four pulses of stimulation are applied to each electrode in turn. The foot
310 response is monitored for short periods after each stimulation, if there is a detectable response it is added to the
311 list of candidate sites. Again the current is automatically adjusted until between 4 and 12 sites are found or the
312 maximum current limit is reached. These sites are ranked in order of sensitivity using a cost function based on
313 the angular displacement. The first two stages therefore allowed for rapid identification of the most sensitive
314 VEs.

315 In phase three (tetanic testing), up to 8 of the sites identified in phase two were tested in rank order with an
316 increasing stimulation intensity. Stimulation began at the level identified in phase two and incremented in steps
317 until one of the following conditions were met: either plantarflexion was corrected to neutral dorsiflexion; or
318 current reaching twice the starting value; or 150% of starting value with no movement detected; or motion
319 saturation was detected. The algorithm included safeguards if unexpected movements occurred, enabling the
320 system to temporarily wait if a leg spasm was detected or to pause the search process if repeated non-stimulated
321 leg movement was detected. Once all the candidate sites were assessed, they were given a score based on a
322 three-part cost function, designed to penalise solutions resulting in plantarflexion, excessive inversion or
323 eversion, and high current. If at any point during this phase the user found a site uncomfortable the clinician was
324 able to skip that site. Once the tetanic testing phase was complete the first-ranked site was activated and, after
325 initial testing of the site while sitting, the user then walked using the stimulator: If the foot response or
326 stimulation sensation was not satisfactory it could be manually changed to an alternative site the ranking list.

327 Finally, stimulus pulse width could be adjusted by the user, if necessary, to fine-tune the magnitude of foot
328 response.

329 4.3 Laboratory-based clinical study

330 Ten participants with drop foot due to stroke (ages 53–71 years) and 11 due to MS (ages 40–80 years) were
331 recruited to test the system. Each participant walked twice over 10 m under each of four conditions; a). using
332 their own stimulator setup by themselves; b) using their own stimulator set up by a clinician, c). using ShefStim
333 with automated setup, and d). no stimulation. Outcome measures were walking speed, foot angle at initial
334 contact and the Borg Rating of Perceived Exertion. As described in Heller et al [6], the results showed that
335 when setup using ShefStim subjects' walking speed, dorsiflexion and frontal plane ankle angle at initial contact
336 were all broadly comparable with clinician setup and, apart from walking speed, better than patient setup. The
337 study demonstrated for the first time that fully automated setup of an array stimulator is feasible in a population
338 with drop foot of central origin.

339 5. FIRST TAKE-HOME STUDY OF SHEFSTIM

340 A final iteration of the stimulator design resulted in the CE- marked ShefStim system shown below.



341

342 *Figure 5: ShefStim stimulator (left) being used by a subject during setup (right)*

343

344 The ShefStim stimulator measures 142mm x 50mm x 14mm (volume 99cc) and weighs 125 g (including
345 batteries). In contrast to the earlier versions of the system, it includes a combined foot angle sensor and remote
346 control device, and setup does not involve holding the leg in a brace (Figure 5). The remote control device is
347 placed on the foot during set up and wirelessly provides triaxial accelerometer inputs to the search algorithm
348 described in the previous section. Users are provided with an attachment, based on an iPod holder, which could
349 be slipped onto the shoe prior to setup. Guidance is provided to the users on the correct mounting of the remote
350 control on the shoe and the importance of aligning the ShefStim box with the long axis of the leg. Once setup is
351 completed, the foot angle sensor device serves as a remote control with which the user can pause stimulation,
352 adjust intensity or receive audible error messages. Stimulation timing during gait is controlled using a
353 conventional footswitch, located under the heel of the shoe. Integrating the foot angle sensor into the system
354 enabled the stimulator to carry out the automated setup routine without requiring input from any external
355 sensors or connection to a PC, making it suitable for use in the home environment.

356 In the final clinical study seven subjects with drop foot (3 subjects with MS, 3 with stroke and 1 with traumatic
357 brain injury) used ShefStim over a 2 week period. The reader is referred to [7] for the experimental protocol and
358 full results. Log data showed that all subjects were able to setup the stimulator outside of the laboratory
359 environment without technical support. Automated setup time averaged 9 minutes, plus 5 minutes to don the
360 equipment. Despite the challenges associated with unsupervised use, including the need for users to correctly
361 align the ShefStim, placed in a pocket of a leg-mounted sleeve, and the remote on their shoe, walking speed and foot
362 response with ShefStim, evaluated in a gait laboratory at the end of the 2 week period showed results
363 comparable with the previous study by Heller [6]. The study demonstrated, for the first time, that array-based
364 automated setup FES system for foot-drop can be successfully used without technical support outside of the
365 laboratory environment.

366 6. DISCUSSION AND CONCLUSIONS

367 The work presented in this paper describes the evolution of the ShefStim design from initial concept in 2003 to
368 evaluation of the CE-marked system by people with stroke in their own homes. A number of issues are worth
369 discussing before conclusions are drawn on the revisions needed to be made to the design.

370 In section 2 we introduced two models used for the identification of electrode array geometry. The activation
371 area is similar in concept to the measure used by Kuhn et al [29], who based their measure of selectivity on an
372 activation volume. As our model assumes the nerve depth to be known (at 10mm in this case), the cross-
373 sectional area of the stimulation pool at 10mm is the measure of the selectivity of stimulation. The larger this
374 area is, the less selective the array stimulation is (i.e. the worse the ability to selectively stimulate neural
375 structures). There are a number of limitations with the model, including the prismatic geometry and assumptions
376 regarding the nerve depth, which undoubtedly varies significantly between subjects. Further, in contrast to Kuhn
377 et al. [29], we did not experimentally validate the model. However, the array geometry and hydrogel properties
378 derived using the model proved to be similar to the array design successfully used in the final take-home study.

379 Although the ShefStim stimulator has been CE marked, there remain a small number of barriers to clinical
380 uptake. By far the most significant of these is that sweat ingress to the hydrogel electrode interface layer leads to
381 a significant drop in its resistivity and an inevitable decay in focality and stimulation efficiency with wear time
382 [30]. These effects limit use of a given array to around one day of continuous wear. In the final study of
383 ShefStim [7] we were able to provide participants with sufficient arrays to use a fresh hydrogel layer each day.
384 However, the cost of such an approach is high and not a realistic solution in clinical practice. To address this we
385 are exploring alternative solutions, including the use of dry electrodes (see, for example [31]). Other minor
386 product development issues remain, including the development of an improved garment to house the stimulator
387 on the leg and minor improvements to the firmware, all of which may be easily resolved. We believe that these
388 improvements would lead to a significant reduction in setup time, as recorded in our final (unsupervised) study
389 [7].

390 In conclusion, this paper has described the complete design, development and evaluation of an array-based FES
391 system with automated setup for the correction of drop foot. The results demonstrate that an array-based
392 stimulator with automated setup is a viable alternative to a conventional surface stimulator, or an implanted
393 stimulator, for the correction of drop foot. Longer term clinical exploitation of ShefStim is dependent on
394 identifying an acceptable alternative to the high-resistivity hydrogel electrode-skin interface layer.

395 **Acknowledgements**

396 This is a summary of independent research funded by the National Institute for Health Research (NIHR) under
397 its Invention for Innovation (i4i) Programme (grant ref HTD480), UK Overseas Research Studentship and
398 Sheffield Hospitals Charitable Trust. The views expressed are those of the author(s) and not necessarily those of
399 the NHS, the NIHR or the Department of Health, or other funding bodies.

400
401
402
403 [1] NICE. Functional electrical stimulation for drop foot of central neurological origin.
404 National Institute for Clinical Excellence; 2009. p. 2.

405 [2] Bosch PR, Harris JE, Wing K, American Congress of Rehabilitation Medicine Stroke
406 Movement Interventions S. Review of therapeutic electrical stimulation for dorsiflexion assist
407 and orthotic substitution from the American Congress of Rehabilitation Medicine stroke
408 movement interventions subcommittee. Arch Phys Med Rehabil. 2014;95:390-6.

409 [3] Roche A, Laighin G, Coote S. Surface-applied functional electrical stimulation for
410 orthotic and therapeutic treatment of drop-foot after stroke -- a systematic review. Physical
411 Therapy Reviews. 2009;14:63-80.

412 [4] Taylor PN, Burridge JH, Dunkerley AL, Lamb A, Wood DE, Norton JA, et al. Patients'
413 perceptions of the Odstock Dropped Foot Stimulator (ODFS). Clin Rehabil. 1999;13:439-46.

414 [5] Melo PL, Silva MT, Martins JM, Newman DJ. Technical developments of functional
415 electrical stimulation to correct drop foot: sensing, actuation and control strategies. Clin
416 Biomech (Bristol, Avon). 2015;30:101-13.

417 [6] Heller BW, Clarke AJ, Good TR, Healey TJ, Nair S, Pratt EJ, et al. Automated setup of
418 functional electrical stimulation for drop foot using a novel 64 channel prototype stimulator
419 and electrode array: results from a gait-lab based study. Med Eng Phys. 2013;35:74-81.

- 420 [7] Prenton S, Kenney LP, Stapleton C, Cooper G, Reeves ML, Heller BW, et al. Feasibility
421 study of a take-home array-based functional electrical stimulation system with automated
422 setup for current functional electrical stimulation users with foot-drop. *Arch Phys Med*
423 *Rehabil.* 2014;95:1870-7.
- 424 [8] BurrIDGE JH, Haugland M, Larsen B, Pickering RM, Svaneborg N, Iversen HK, et al.
425 Phase II trial to evaluate the ActiGait implanted drop-foot stimulator in established
426 hemiplegia. *J Rehabil Med.* 2007;39:212-8.
- 427 [9] Kottink AI, Hermens HJ, Nene AV, Tenniglo MJ, van der Aa HE, Buschman HP, et al. A
428 randomized controlled trial of an implantable 2-channel peroneal nerve stimulator on walking
429 speed and activity in poststroke hemiplegia. *Arch Phys Med Rehabil.* 2007;88:971-8.
- 430 [10] Merson E, Swain I, Taylor P, Cobb J. Two-channel stimulation for the correction of drop
431 foot. 5th Conference of IFESS UK & Ireland. Sheffield, UK2015.
- 432 [11] Seel T, Werner C, Raisch J, Schauer T. Iterative learning control of a drop foot
433 neuroprosthesis - Generating physiological foot motion in paretic gait by automatic feedback
434 control. *Control Eng Pract.* 2016;48:87-97.
- 435 [12] Seel T, Valtin M, Werner C, Schauer T. Multivariable Control of Foot Motion During
436 Gait by Peroneal Nerve Stimulation via two Skin Electrodes. 9th IFAC Symposium on
437 Biological and Medical Systems. Berlin, Germany2015.
- 438 [13] Whitlock T, Peasgood W, Fry M, Bateman A, Jones R. Self-optimising electrode arrays.
439 5th IPEM Clinical Functional Electrical Stimulation Meeting. Salisbury1997.
- 440 [14] Elsaify E, Fothergill J, Peasgood W. A portable FES system incorporating an electrode
441 array and feedback sensors. 8th Vienna International workshop functional electrical
442 stimulation. Vienna, Austria2004.
- 443 [15] Hernandez JD. Development and Evaluation of a Surface Array Based System to Assist
444 Electrode Positioning in FES for Drop Foot: University of Surrey; 2009.
- 445 [16] Kuhn A, Keller T, Micera S, Morari M. Array electrode design for transcutaneous
446 electrical stimulation: a simulation study. *Med Eng Phys.* 2009;31:945-51.
- 447 [17] Valtin M, Steel T, Raisch J, Schauer T. Iterative learning control of drop foot stimulation
448 with array electrodes for selective activation. 19th World Congress IFAC. Cape Town, South
449 Africa2014.
- 450 [18] Hernandez MD. Development and evaluation of a surface array based system to assist
451 electrode positioning in FES for drop foot: University of Surrey; 2009.
- 452 [19] Kenney L, Heller B, Barker AT, Reeves M, Healey J, Good T, et al. The Design,
453 Development and Evaluation of an Array-Based FES System with Automated Setup for the
454 Correction of Drop Foot. 9th IFAC Symposium on Biological and Medical System. Berlin,
455 Germany2015.
- 456 [20] Heller B, Barker AT, Sha N, Newman J, Harron E. Improved control of ankle movement
457 using an array of mini-electrodes. FES User Day Conference. Birmingham, U.K.2003.
- 458 [21] Sha N, Heller BW, Barker AT. 3D modelling of a hydrogel sheet - electrode array
459 combination for surface functional electrical stimulation. Proceedings of the 9th Annual
460 Conference of IFESS. Bournemouth, UK2004. p. 431-3.
- 461 [22] Duck FA. Physical properties of tissue : a comprehensive reference book. London:
462 Academic Press; 1990.
- 463 [23] Rattay F. Analysis of models for external stimulation of axons. *IEEE Trans Biomed Eng.*
464 1986;33:974-7.
- 465 [24] Sha N. Development of a steerable electrode array for functional electrical stimulation:
466 Sheffield University; 2003.
- 467 [25] Sha N, Kenney LP, Heller BW, Barker AT, Howard D, Wang W. The effect of the
468 impedance of a thin hydrogel electrode on sensation during functional electrical stimulation.
469 *Med Eng Phys.* 2008;30:739-46.

- 470 [26] Sha N, Kenney LP, Heller BW, Barker AT, Howard D, Moatamedi M. A finite element
471 model to identify electrode influence on current distribution in the skin. *Artif Organs*.
472 2008;32:639-43.
- 473 [27] Sha N. A surface electrode array-based system for functional electrical stimulation:
474 University of Salford; 2009.
- 475 [28] Woodburn J, Helliwell PS, Barker S. Three-dimensional kinematics at the ankle joint
476 complex in rheumatoid arthritis patients with painful valgus deformity of the rearfoot.
477 *Rheumatology* (Oxford, England). 2002;41:1406-12.
- 478 [29] Kuhn A, Keller T, Lawrence M, Morari M. The influence of electrode size on selectivity
479 and comfort in transcutaneous electrical stimulation of the forearm. *IEEE Trans Neural Syst*
480 *Rehabil Eng*. 2010;18:255-62.
- 481 [30] Cooper G, Barker AT, Heller BW, Good T, Kenney LP, Howard D. The use of hydrogel
482 as an electrode-skin interface for electrode array FES applications. *Med Eng Phys*.
483 2011;33:967-72.
- 484 [31] Yang K, Freeman C, Torah R, Beeby S, Tudor J. Screen printed fabric electrode array
485 for wearable functional electrical stimulation. *Sensor Actuat a-Phys*. 2014;213:108-15.
486

A review of the design and clinical evaluation of the ShefStim array-based functional electrical stimulation system.

Laurence P. Kenney^{*1}, Ben W. Heller², Anthony T. Barker³, Mark L. Reeves³, Jamie Healey³, Timothy R. Good³, Glen Cooper^{1,4}, Ning Sha¹, Sarah Prenton^{1,5}, Anmin Liu¹, David Howard¹

¹Centre for Health Sciences Research, University of Salford, Salford M6 6PU, U.K.

²Centre for Sports Engineering Research, Sheffield Hallam University, Sheffield S1 1WB, U.K.

³Department of Medical Physics and Clinical Engineering, Royal Hallamshire Hospital, Sheffield S10 2JF U.K.

⁴School of Mechanical, Aerospace and Civil Engineering, University of Manchester, Manchester, M13 9PL, U.K.

⁵Division of Health and Rehabilitation, University of Huddersfield, Huddersfield HD1 3DH, U.K.

* Corresponding author: email - l.p.j.kenney@salford.ac.uk; tel 0161295 2289

Abstract: Functional electrical stimulation has been shown to be a safe and effective means of correcting foot drop of central neurological origin. Current surface-based devices typically consist of a single channel stimulator, a sensor for determining gait phase and a cuff, within which is housed the anode and cathode. The cuff-mounted electrode design reduces the likelihood of large errors in electrode placement, but the user is still fully responsible for selecting the correct stimulation level each time the system is donned. ~~Over recent years~~ Researchers have investigated different approaches to automating aspects of setup and/or use, including recent promising work based on iterative learning techniques. This paper reports on the design and clinical evaluation of an electrode array-based FES system for the correction of drop foot, ShefStim. The paper reviews the design process from proof of concept lab-based study, through modelling of the array geometry and interface layer to array search algorithm development. Finally, the paper summarises two clinical studies involving patients with drop foot. The results suggest that the ShefStim system with automated setup produces results which are comparable with clinician setup of conventional systems. Further, the final study demonstrated that patients can use the system without clinical supervision. ~~Although w~~When used unsupervised, ~~setup time was found to be 14 minutes (relatively long (9 minutes for automated search plus 5 minutes for donning the equipment), although this figure cannot be directly compared with other systems, which have reported setup time from purely lab-based could be reduced studiessignificantly with relatively minor changes to the design.-~~

1. INTRODUCTION

Functional electrical stimulation has been shown to be a safe and effective means of correcting foot drop of central neurological origin [1-3]. Surface-based devices typically stimulate via a cathode placed over the common peroneal nerve ~~close immediately distal~~ to where it bifurcates into the deep and superficial branches, and an anode placed over tibialis anterior. Appropriate levels of stimulation delivered via accurately placed electrodes should result in suitably weighted recruitment of the two nerve branches, leading to a useful and safe foot response during the swing phase of walking (dorsiflexion with a small degree of eversion). However, in certain individuals even very small electrode positioning errors can lead to a poor foot response. Indeed, a 1999 survey of users of drop foot stimulators ~~over-reported over~~ 40% of respondents ~~reported~~ finding electrode positioning problematic [4] [2]. ~~Modern~~ Some current systems ~~(the reader is referred to [5] for a recent review paper)~~, such as the WalkAide (Innovative Neurotronics Inc., Austin, Texas, USA) embed electrodes in a cuff, worn below the knee ~~(the reader is referred to [5] for a recent review of current systems)~~. ~~Such an approach which~~ greatly reduces the likelihood of large errors in electrode placement, but the user is still fully responsible for selecting the correct stimulation level each time the system is donned. ~~The reader is referred to a recent review of drop foot stimulator technologies for an overview of commercial and other systems [5]~~. Interestingly, despite improvements in both stimulator designs and patient education, two recent studies demonstrated that when patients set up their stimulators without clinician support, the resultant foot response is often less than optimal [3,4][6, 7].

One approach to the challenge of stimulator setup is to implant the electrodes on the nerve(s), thereby removing the electrode placement problem from the user [5,6][8, 9]. However, an invasive approach carries risks and the implantable devices and surgical costs remain relatively expensive. As a result, a number of groups have been investigating the possibility of automating the surface-based drop foot setup process through ~~using~~ a two-channel stimulation approach to software steering of the foot [10-12][7,8], or electrode array-based approaches

53 ~~[9-12][13-18]. Both approaches aim to de-skill the physical electrode placement and setup process, which in~~
54 ~~turn may lead to improved, and more consistent foot responses. Both approaches rely on a method for~~
55 ~~'opening up the search-setup space' which can be automatically searched, either through replacing single~~
56 ~~electrode(s) with one or two arrays of discrete electrodes, or by allowing modulation of manipulating pulse~~
57 ~~waveform. Both approaches also use feedback-measurement of a foot pose/orientation, usually derived from~~
58 ~~foot-worn inertial sensors, to guide the search.~~

59 ~~The replaces an electrode array replaces the single stimulating electrode used with conventional surface FES.~~
60 ~~Each electrode in the array can be independently activated and used to deliver stimulation to localized areas.~~
61 ~~Simultaneous activation of several neighbouring electrodes can be used to form a virtual stimulating electrode or~~
62 ~~virtual electrode (VE). Such an approach opens up the potential of software selection of the size, shape and~~
63 ~~position of the virtual electrode without physical re-location of the electrode array and hence the automation of~~
64 ~~the (virtual) electrode positioning process. Elsaify proposed an automatic array element search algorithm, but~~
65 ~~using array elements with separate gel layers (a matrix of small single electrodes) were used [14]. More~~
66 ~~recently, Valtin [17] demonstrated an array search algorithm that takes roughly two minutes, using two flexible~~
67 ~~PCB electrode arrays (one over the nerve and one over Tibialis Anterior), each interfaced with a continuous,~~
68 ~~high-resistivity hydrogel layer. However, in contrast to the work presented here, only preliminary results with a~~
69 ~~healthy subject were presented. In the most recent work, Seel reported on a system using a foot-mounted inertial~~
70 ~~sensor to adjust the steering based on realtime measurements of the foot orientation [11]. The system uses only~~
71 ~~two electrodes and, in laboratory studies with stroke participants, demonstrates convergence on a suitable foot~~
72 ~~response within one or two strides. However, studies of the system outside of the laboratory setting have yet to~~
73 ~~be published.~~

74 ~~In this paper we expand on a recent conference paper [13][19] to report on the design, development and~~
75 ~~demonstration of a system for automated setup of drop foot FES (ShefStim). The paper extends the work~~
76 ~~presented in the conference paper by presenting the model used to define the initial a detailed description of the~~
77 ~~electrode array geometry design problem (section 2) and provides discussion of the merits and limitations of~~
78 ~~ShefStim compared with alternative systems. by xxx.~~

79 ~~Following a review of the design and development process, results from world first demonstrations of an array-~~
80 ~~based system for drop foot in clinical groups, first in the laboratory and then unsupervised in community~~
81 ~~settings, are summarised. Finally, the plans for future work are discussed. The ShefStim design concept was~~
82 ~~proposed by Heller in 2003 [14][20]. In this approach an electrode array replaces the single stimulating~~
83 ~~electrode used with conventional surface FES. Each electrode in the array can be independently activated and~~
84 ~~used to deliver stimulation to localized areas. Simultaneous activation of several neighbouring electrodes can be~~
85 ~~used to form a virtual stimulating electrode or virtual electrode (VE). Such an approach opens up the potential of~~
86 ~~software selection of the size, shape and position of the virtual electrode without physical re-location of the~~
87 ~~electrode array and hence the automation of the (virtual) electrode positioning process.~~

88 ~~For this study the Department of Medical Physics at Sheffield Teaching Hospitals initially developed a~~
89 ~~'proof-of-concept' multi-electrode stimulator, which. This device could simultaneously stimulate any manually-~~
90 ~~selected subset out of a conveniently sized, 8 by 8 rectangular array of metal electrodes. The subset of activated~~
91 ~~electrodes is termed a virtual electrode (VE). In order to develop this concept into a clinically usable system for~~
92 ~~automated setup a series of design problems needed to be solved. These are addressed in turn, below. The first~~
93 ~~problem was the electrode array design; the second problem was the development of an array search algorithm.~~
94 ~~The remaining part of the paper summarises the results from two studies of the ShefStim involving people with~~
95 ~~drop foot of central neurological origin.~~

97 2. SHEFSTIM DESIGN CONCEPT

98 ~~The ShefStim design concept was proposed by Heller in 2003 [14]. In this approach an electrode array replaces~~
99 ~~the single stimulating electrode used with conventional surface FES. Each electrode in the array can be~~
100 ~~independently activated and used to deliver stimulation to localized areas. Simultaneous activation of several~~
101 ~~neighbouring electrodes can be used to form a virtual stimulating electrode or virtual electrode (VE). Such an~~
102 ~~approach opens up the potential of software selection of the size, shape and position of the virtual electrode~~
103 ~~without physical re-location of the electrode array and hence the automation of the (virtual) electrode~~
104 ~~positioning process.~~

105 ~~The Dept. of Medical Physics at Sheffield Teaching Hospitals initially developed a 'proof-of-concept' multi-~~
106 ~~electrode stimulator. This device could simultaneously stimulate any manually-selected subset out of a~~
107 ~~conveniently sized, 8 by 8 rectangular array of metal electrodes. In order to develop this concept into a clinically~~

108 | ~~usable system for automated setup a series of design problems needed to be solved. These are addressed in turn,~~
109 | ~~below.~~

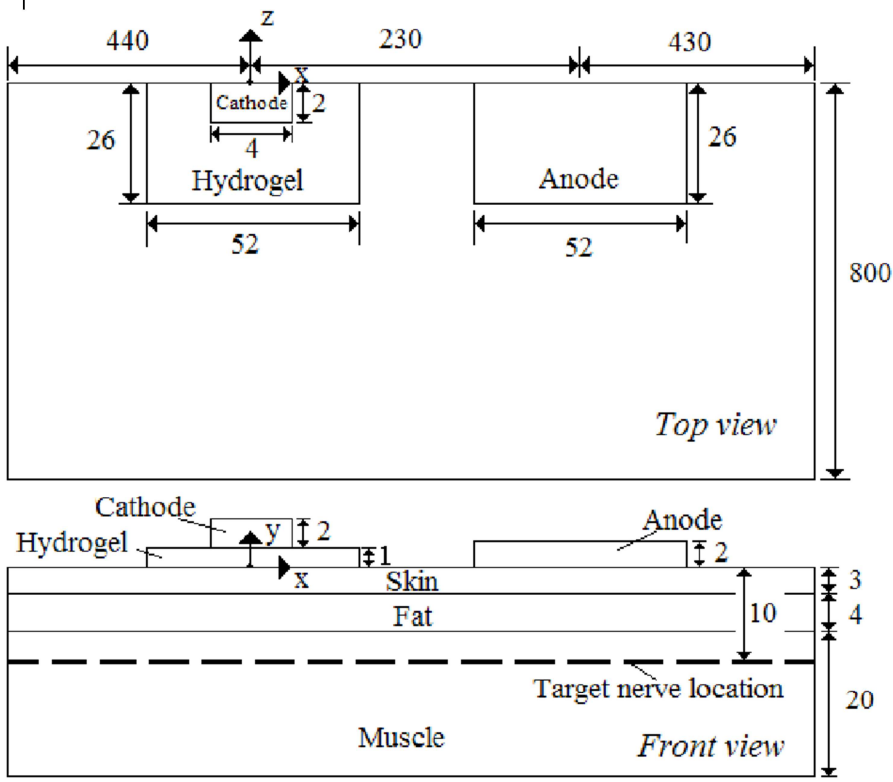
110 | 3.2. DESIGN OF THE ELECTRODE ARRAY

111 | For clinical applications a moderately electrically conductive hydrogel interface between the electrodes and skin
112 | provides ~~increased comfort,~~ the benefits of hydration of, and adhesion to, the skin. However, in array
113 | applications a continuous hydrogel layer also introduces the issue of spatial selectivity loss due to transverse
114 | currents in the hydrogel. Spatial selectivity is defined as the ability to activate discrete groups of nerve fibres in
115 | a localised region without stimulating nerve fibres in neighbouring regions.

116 | In order to achieve a satisfactory degree of spatial selectivity, it was necessary to identify an appropriate
117 | electrode geometry and interface layer properties. Two finite-element models were therefore developed to
118 | investigate the effects of electrode geometry and hydrogel layer properties on spatial selectivity, characterised in
119 | our model by the activation area (see below). Model 1 was developed to explore the effects of hydrogel
120 | resistivity and electrode size on ~~spatial selectivity~~ activation area under a single cathode electrode and; Model 2
121 | extended Model 1 through the addition of a number of electrodes surrounding the cathode, to allow investigation
122 | of ~~spatial selectivity~~ activation area under a multi-electrode array. The results of the second model, together with
123 | practical constraints imposed by the stimulator, led to the array geometry and interface layer properties used in
124 | part 4.3 of this paper.

125 | *Model 1*

126 | [Figure 1](#) shows ~~Athe~~ 3D finite ~~element~~ model, ~~was~~ developed using ANSYS Multiphysics (Version 10.0,
 127 | Ansys, Inc, Canonsburg, PA, USA) to predict the effects of electrode geometry and hydrogel properties on
 128 | electric field distribution in the underlying tissue [\[15\]](#)[21]. The model represented ~~sed~~ a cathode, an anode, a
 129 | hydrogel layer, skin, fat and muscle. The skin, fat and muscle were modelled as flat, extended layers, whose
 130 | thicknesses were based on their anatomical dimensions. [As bone has much higher resistivity than the other](#)
 131 | [media, it was assumed to be non-conductive volume underlying the muscle, and hence was represented as the](#)
 132 | [lower boundary of the model. Structures of smaller dimension, such as hair follicles or blood vessels, were not](#)
 133 | [explicitly modelled, as their influence on stimulation at the depth of the motor nerve branches could be](#)
 134 | [considered negligible.](#)
 135 | Appropriate electrical conductivity properties were assigned to the elements, [based on values from Duck](#) [22]
 136 | [\(Table 1\). Time was not represented, as the electrical properties were assumed to be dominated by resistance.](#)
 137 | [Although the skin's capacitance cannot normally be neglected, the skin in the model was assumed to be](#)
 138 | [hydrated due to intimate contact with the hydrogel layer. Hence capacitive effects were not included in this](#)
 139 | [model.](#)



140 | [Figure 1: Schematic of the geometry of the selectivity FE model \(not to scale\) \(dimensions inmm\)](#)
 141 |

142 | [Table 1: Model parameters](#)
 143 |

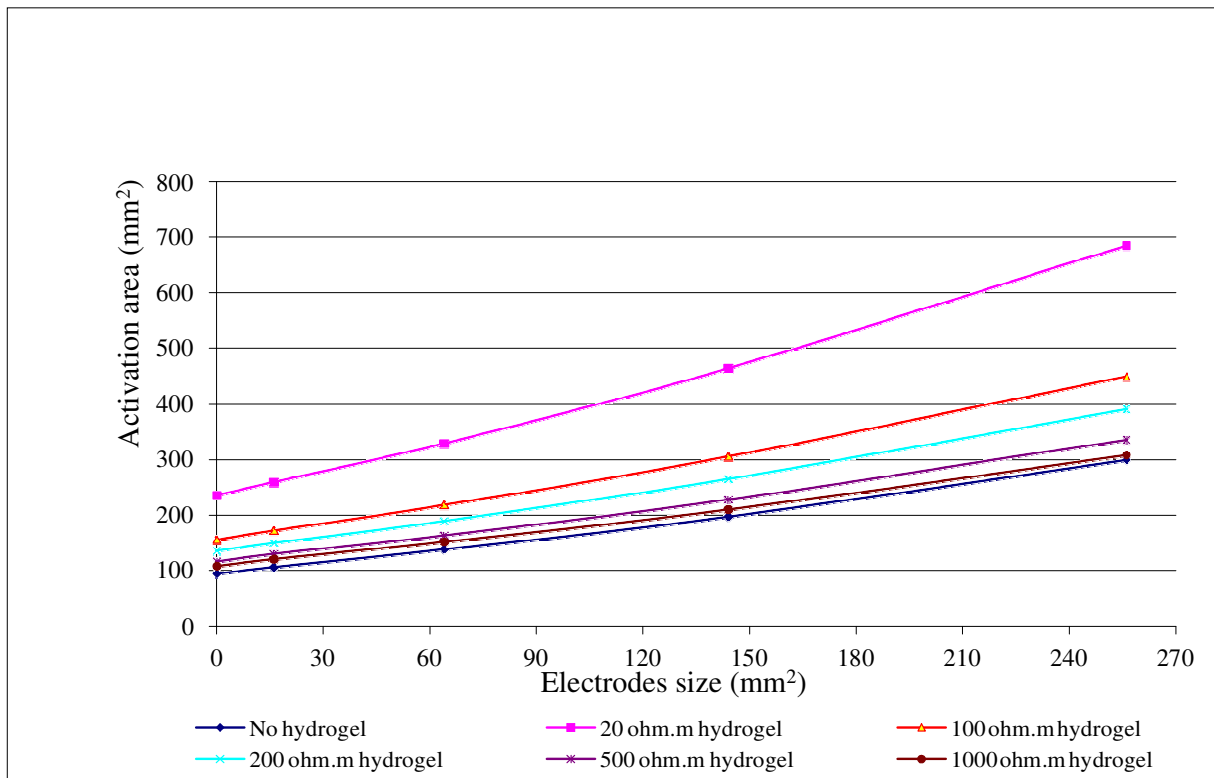
Biological tissues and materials	Resistivity (Ωm)
Bone	7×10^4
Muscle	2 in X and Z directions
	4 in Y direction
Fat	62.5
Skin (hydrated)	833
Hydrogel	Model variable
Cathode and Anode	1.5×10^{-8}

144 |

145 The calculation of whether a point in the model was deemed to be stimulated was based on the stimulation
 146 function [16][23]. To explore spatial selectivity we first defined a stimulus pool to be a volume over which
 147 the value of the stimulation function exceeds a threshold at which action potentials in a nerve fibre are generated.
 148 The maximum stimulation function always appears in the stimulus pool centre, just underneath the cathode,
 149 and the amplitude of the stimulation function decreases from the centre to the edge of the stimulus pool.
 150 Although the value of the maximum stimulation function varies between models, it can always be scaled to the
 151 same value by changing the input current, and this scaling does not change the shape or size of the stimulus
 152 pool. Contours may be defined which connect points in the model with identical stimulation function values
 153 (expressed as a percentage of the maximum) and the 50% contour was selected to represent the boundary of the
 154 stimulus pool for the results presented here. The 50% contour choice was somewhat arbitrary, but avoided
 155 problems which would be associated with choice of a contour near 100% or 0% of maximum stimulation
 156 function (all contours converge to a point at 100% of maximum stimulation function and contours enclose
 157 infinitely large areas at 0%). For brevity in the results presented in this paper we consider only a stimulus pool
 158 representing 50% of the maximum stimulation function (readers are referred to [17] for more details). As the
 159 electrical properties of the tissue were uniform, the current density distribution was symmetric along the plane
 160 normal to the skin surface and along the centres of the cathode and the anode. This symmetry allowed a study to
 161 be performed on a half model. To represent the location of the nerve, we defined a plane representing the
 162 anatomical depth of the target nerve (10mm). The intersection of the stimulus pool with the plane defined an
 163 area; the smaller the area, the more focused is the stimulation and thus the better the spatial selectivity.
 164 Therefore, the area of the stimulus contour associated with 50% of maximal stimulation was used as the metric
 165 of spatial selectivity.

166 To explore the combined effect of hydrogel resistivity and electrode size on selectivity, a series of simulations
 167 were run with square electrodes from infinitely small (a point) to 16mm×16mm with a range of interface layers.
 168 The first simulation considered the no interface layer case; subsequent simulations varied the 1mm thick
 169 hydrogel layer resistivity from 20Ωm to 1000Ωm. The results are shown in Figure 1.

170



171

172 Figure 21: The effects of electrode size on spatial activation area selectivity for a range of hydrogel resistivities.

173

174

175 | Figure 1 shows that [there is a minimum limit to activation area of approximately 100mm² at 10mm depth, and](#)
 176 | [that spatial selectivity becomes poorer \(selectivity-coefficientactivation area increases\)](#) with increasing size of
 177 | electrode and decreasing resistivity. When the resistivity reaches 500Ωm or [moregreater](#), the spatial selectivity
 178 | is similar to that of the model without the hydrogel sheet.

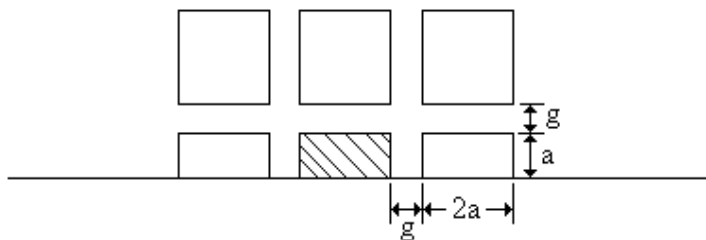
179 | *Model 2*

180 | Model 1 had shown that the introduction of a 1 mm hydrogel interface layer did not significantly degrade
 181 | selectivity providing the hydrogel resistivity was at least 500Ωm. However, the model did not account for the
 182 | presence of neighbouring electrodes which would surround an electrode in the array. The presence of these
 183 | electrodes [may-will](#) lead to a decrease in selectivity compared with the single electrode condition, as current can
 184 | flow from activated electrodes across inter-electrode gaps and into adjacent non-activated electrodes. These
 185 | effects would be modulated by the size of the inter-electrode gap and hydrogel properties. Therefore, Model 1
 186 | was used as the basis for a new model (Model 2) to enable the electrode array design to be finalised.

187 | It was assumed that the magnitude of reduction in selectivity due to current passing across the inter-electrode
 188 | gaps would be dominated by electrodes immediately surrounding any given electrode in the array. Hence,
 189 | Model 1 was extended to include eight more electrodes surrounding the original cathode electrode ([Figure 2](#))¹.
 190 | The interface between the electrode array and the skin was a sheet of hydrogel. The initial geometry of Model 2
 191 | [were-was](#) informed by previous pilot experimental work [carried out as part of a Master's research project,](#)
 192 | demonstrating the viability of using a 70mm x70mm electrode array consisting of 64 electrodes (arranged in an
 193 | 8x8 format)[24].

194 |

195 |



196 | surrounding electrodes the stimulating electrode

197 | *Figure 332: Model 2. The electrode gap (g) is the edge-to-edge distance between any two neighbouring electrodes in the*
 198 | *array; 2a is the dimension of each square electrode*

199 | As the feasibility work suggested maintaining an overall array size of approximately 70mm x 70mm , we fixed
 200 | the centre-to-centre spacing of electrodes in the model to be 9mm (2a + g =9, see [Figure 2](#)). Five different gap
 201 | sizes were modelled ([Table 1](#)) and for each of these, four commercial hydrogel sheets were modelled ([Table](#)
 202 | [2](#)). The set of hydrogel properties were informed not only by the results of Model 1, but also by earlier
 203 | experimental work [\[18,19\]](#)[25, 26] which provided further evidence to support the use of a thin, high-resistivity
 204 | hydrogel layer between the electrode and skin.

205 | *Table 224: Electrode gap and size evaluated in the FE model, and resultant overall electrode array size*

Electrode gap (mm)	Electrode size (mm)	Electrode array size (mm)
1	8×8	71×71
2	7×7	70×70
3	6×6	69×69
4	5×5	68×68
5	4×4	67×67

¹ Note, as per Model 1, a half model was developed to take advantage of symmetry.

206
207
208

Table 332: Hydrogel materials represented in the model. Note that the different sheet thicknesses modelled were chosen to represent the sheet thicknesses provided by the manufacturers.

Hydrogel (abbreviation)	Approx thickness (mm)	Resisitivity at 1.67kHz (Ωm)
AG703, Axelgaard manufacture Co., Ltd. Fallbrook, CA. USA (Hydrogel 703)	0.9	55
AG803, Axelgaard manufacture Co., Ltd. Fallbrook, CA. USA (Hydrogel 803)	0.9	206
SRBZAB-05SB, Sekisui Plastics, Co., Ltd. Tokyo, Japan (Hydrogel ST)	0.5	1363
AG, AG3AM03M-P10W05, Sekisui Plastics, Co., Ltd. Tokyo, Japan (Hydrogel AG)	0.3	25185

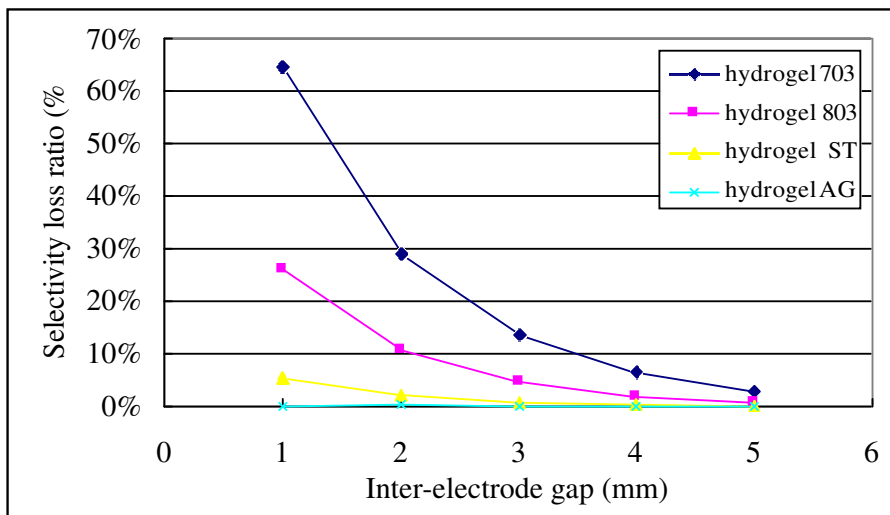
209

210 In order to quantify the effects of the surrounding electrodes on selectivity, two versions of each model were
211 run. In the first version, the surrounding electrodes were not represented and in the second, the surrounding
212 electrodes were represented. The selectivity loss resulting from the introduction of surrounding electrodes was
213 quantified by a selectivity loss ratio, defined in equation 1.

214
$$\text{Selectivity_loss_ratio} = \frac{A_2 - A_1}{A_1} \times 100\% \quad (1)$$

215 Where, A_1 is the ~~selectivity coefficient~~ activation area of the model without surrounding electrode and A_2 is
216 the ~~selectivity coefficient~~ activation area of the model with surrounding electrode
217

218 Figure 3 shows the selectivity loss ratio due to the surrounding electrodes calculated for each combination of
219 hydrogel interface layer and inter-electrode gap.
220



221
222

Figure 3: Selectivity loss ratios with different hydrogels

223 The results suggested that for hydrogels ST and AG an electrode gap between 1mm and 5mm will result in an
224 acceptably low selectivity loss (defined as less than 10%) in the presence of the surrounding electrodes. From a
225 manufacturing perspective, an inter-electrode gap of less than 2mm would make it very difficult to route the
226 tracks between electrodes, so a 2mm inter-electrode gap was chosen. A final practical test demonstrated that our

227 stimulator (200V drive voltage) could not drive the specified 8mA per channel when using the more resistive of
228 the two most promising materials (hydrogel AG) and hence hydrogel ST was selected.

229 4.3. FEASIBILITY STUDY OF ELECTRODE ARRAY SEARCH STRATEGY

230 Section 3 described the design of an 8 x 8 electrode array interfaced to the skin via a thin high-resistivity
231 hydrogel layer. The next design problem was the development of a quick, reliable method of searching the set of
232 all possible stimulation electrodes to find the optimal virtual electrode. ~~Prior to this work, Elsaify et al [10] had~~
233 ~~already shown promising results using foot twitch response, the response of the muscle to a single stimulation~~
234 ~~pulse, in their search of an electrode array.~~ In this section we report on two methods for searching the array
235 used to identify appropriate virtual electrodes and their associated stimulation levels, which extended the work
236 of Elsaify et al. [10]–[14]. In the first part of the work, we apply a slowly ramped stimulation through each
237 virtual electrode while continuously monitoring the orientation of the foot relative to the leg. These data allow
238 identification of electrode sets that, when appropriately stimulated, result in acceptable foot movement. The
239 ramped stimulation results were used to investigate whether it is possible to reduce the search space through
240 prediction of the location of the best subset of these electrodes based only on the response of the foot to short
241 bursts of stimulation (twitch stimulation). We investigated use of a cost function to rank the response to short
242 bursts of stimulation and examine whether this ranking may be used to isolate smaller groups of electrodes that
243 contain one or all of the best subset of electrodes identified in the slow ramped stimulation search.

244 For brevity, here we only report on the search for appropriate single VEs. Additional work to identify suitable
245 pairs of VEs is reported elsewhere [17][27]. Ethical approval for the study was granted by the University of
246 Salford's Research Governance and Ethics committee (RGE06/102). Twelve healthy subjects were recruited
247 from within the University and a full set of results were obtained for ten (9 male) subjects (median 30 years)².

248 The stimulation system consisted of a constant current portable 64 channel stimulator designed and built by the
249 Medical Engineering section of Sheffield Teaching Hospitals NHS Foundation Trust (size: 155 mm × 95 mm ×
250 33 mm), an 8x8 electrode array, described in section 3.2 and a 50x50 mm square conventional hydrogel
251 electrode (PALS® Platinum electrode, Axelgaard Manufacturing Co. Ltd.). The charge-balanced asymmetrical
252 biphasic stimulus pulses were software controllable via a graphical user interface, with the pulse width fixed at
253 300 μs, and the frequency at 35 Hz. Stimulation intensity through each electrode was software controlled and
254 measured by an analogue to digital converter built-in to the stimulator itself. During the experiment, groups of
255 2x2 electrodes were activated simultaneously (the minimum number required to elicit adequate contractions,
256 providing a total current of up to 32 mA), and act as a virtual electrode.

257
258 A 5-camera Qualisys motion capture system (Proreflex, Qualisys AB, Sweden) was used to record foot
259 movement at 100Hz and the motion data were transferred to and simultaneously analysed in Visual3D
260 (Visual3D™, C-Motion Inc, USA). Hence the foot movement was captured, and ankle angles in sagittal,
261 coronal and transverse planes were displayed in real-time. Synchronisation between the stimulator and the
262 motion capture system was achieved using a data acquisition device via the stimulator control program. An
263 electrically-isolated button was included to allow the user to stop stimulation at any stage in the experiment.

264 The experiment started with measurement of the neutral foot orientation for the subject while standing upright.
265 He/she was then asked to sit in a chair and their right lower leg was strapped in the brackets to keep the shank in
266 a consistent pose throughout. The stimulator and electrodes were then donned. The subject was then asked to
267 maintain their sitting posture and relax the foot in a naturally relaxed (dropped) position throughout the
268 experiments. As the analysis of data did not dictate the order in which the tests were conducted, the foot twitch
269 experiment was conducted first to reduce fatigue. However, here they are explained in reverse order for clarity.

270 Prior to beginning the slow ramped stimulation experiment a user-defined maximal current was identified. We
271 assumed that sensation would be most acute over bony prominences and hence at the start of the experiment
272 increased stimulation over these sites until a user-defined maximum was reached and the value noted. Next,
273 current through each VE in turn was ramped from zero to the user-defined maximal current over 10 seconds.
274 The twitch stimulation part of the experiment involved six different bursts of stimulation (1 and 4 pulses/burst,
275 at 3 different levels of stimulation (16, 24 and 32mA) being applied in turn through each of the 49 VEs. Ankle
276 angles together with time-synchronised current data for each of the different electrodes were recorded for both
277 experiments.

278
279 The target for foot orientation was defined as dorsiflexion at or above neutral, and inversion/eversion within -
280 1SD of the previously reported healthy subject mean foot orientation at heel strike [20][28]. All VEs which,

²Two subjects could only tolerate 12.8 mA and 16 mA respectively, which was insufficient to produce target dorsiflexion when applied through any of the virtual electrodes electrodes during the slowly ramped stimulation

281 when stimulated over the 10 second period, resulted in the foot reaching the target foot orientation were
 282 identified and the set of electrodes satisfying these criteria were labelled Set A.

283
 284 | As can be seen from figure 4, when sitting relaxed in the chair the subject's foot was typically plantarflexed
 285 and inverted, compared with its neutral position. Hence, it was assumed that a twitch response that moved the
 286 foot towards dorsiflexion and eversion was desirable. A cost function was defined which used the maximum
 287 value of dorsiflexion and inversion angles observed during the twitch response

288
 289
$$Cost = -2 \cdot Dorsi + Inver$$

290 Where *Dorsi* is the peak dorsiflexion angle (in degrees) measured during stimulation relative to the relaxed
 291 position. Dorsiflexion is positive and plantarflexion is negative. *Inver* is the peak inversion angle (in degrees)
 292 measured during stimulation relative to the relaxed position. Inversion is positive and eversion is negative. A
 293 weighting factor of 2 was applied to the dorsiflexion angle to reflect its relative importance compared to
 294 inversion/eversion.

295
 296 This cost function was used to rank the foot responses to each of the different twitch stimulation bursts applied
 297 to each of the VEs. The cost function, which was applied to the positive peak value of dorsiflexion and
 298 inversion, maximizes dorsiflexion and minimizes inversion. The VE with the lowest cost was ranked 1st and
 299 each of the remaining 48 VEs were then assigned a rank based on their cost. To identify how well the cost
 300 function could be used to predict membership of Set A (the set of VEs which, when stimulated resulted in the
 301 foot reaching the target foot orientation) two metrics were derived. First, how far down the ranking it was
 302 necessary to go to include all of the members of Set A, defined as Rank_all ; second, how far down the ranking
 303 it was necessary to go to include any member of Set A, defined as Rank_any.

304
 305 In 9 out of the 10 subjects to complete the slow ramped stimulation study, at least 1 VE was identified which,
 306 when stimulated, produced the target foot response. The maximum number of acceptable VEs found for any
 307 individual subject was 4 (out of 49) and the minimum was 0.

308 | The results of the twitch stimulation analysis for the 9 subjects are shown in [Table 34](#). Note that stimulation at
 309 16mA produced no or minimal response.

310
 311 | *Table 443: Rank_any and Rank_all for different twitch stimuli*

	1 pulse @ 32mA	4 pulses @ 32mA	1 pulse @ 24mA	4 pulses @ 24mA
Rank_all Median (range)	5 (1-33)	4 (1-41)	11 (2-40)	8 (2-41)
Rank_any Median (range)	2 (1-19)	3 (1-15)	6 (1-15)	4 (1-29)

312
 313 Although there was significant inter-subject variability, the results showed that in most cases by using a cost
 314 function to rank responses to twitch stimulation it was possible to identify a much smaller set of electrodes
 315 containing one, or all of Set A. For example, using a 4 pulse burst of stimulation at 32mA, a suitable electrode
 316 was identified in all cases within the first 15 of the responses ranked according to the slow ramped stimulation
 317 results. The data suggested therefore there could be advantage to using a twitch stimulation consisting of
 318 multiple pulses at high currents and a two stage search strategy was worth further investigation.

319 | 45. FIRST LAB-BASED DEMONSTRATION OF SHEFSTIM

320 Further development work on both the stimulator and the search algorithm was carried out over the period 2009-
 321 11 resulting in the first demonstration of an array-based FES system with automated setup for the correction of
 322 drop foot. The study is reported in detail elsewhere [6][24], so in this paper, we focus on the improvements

323 made to the stimulator hardware and implementation of the search algorithm, and provide an overview of the
324 laboratory-based study involving subjects with drop foot.

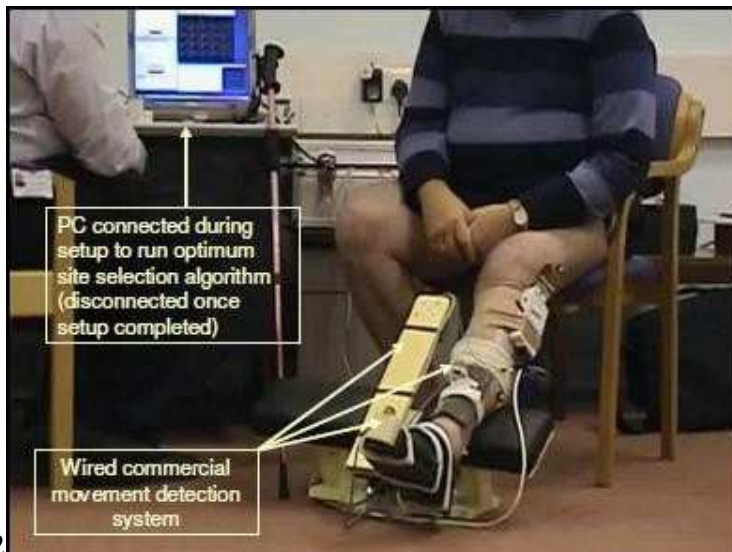
325 [5.14.1](#) Stimulator

326 Further stimulator development led to a new design weighing 200 g with a volume of 211cc (130 mm x 65 mm
327 x 25 mm). During automated setup the stimulator was controlled via an isolated serial link by a program
328 running on an external computer, the participant's leg was held in a brace, with the knee extended and foot
329 movement was measured using an electromagnetic position and orientation sensor (Patriot, Polhemus Inc,
330 Vermont) (~~figure~~ [Figure 4](#)). For walking trials the setup parameters were downloaded and the stimulator
331 disconnected from the computer, enabling it to function as a standalone drop foot stimulator being triggered
332 using a foot switch.

333 [5.24.2](#) Search algorithm

334 The work described in section 4 had been based on the use of a 2 x 2 VE. Following further pilot work it was
335 found that a 4 x 4 VE still provided satisfactory resolution over foot response, but reduced sensation compared
336 to a 2x2 arrangement and increased robustness to tissue movement during gait. The move to a 4 x 4 VE also
337 served to reduce the array search space by a factor of ~2, compared with the original approach. [\(25 VEs to be
338 searched rather than 49\).](#)

339 As described in section 4, we had already demonstrated the potential to use the response of the foot to short
340 bursts of stimulation as a means of homing in on promising VEs. However, further work was needed to develop
341 a clinically usable search algorithm. In the final system a three phase search strategy was implemented.



342
343 *Figure 4: Setup of ShefStim*

344 In phase one the level of stimulation at which the foot first responds is determined. Short bursts of stimulation
345 are applied to each of the 25 virtual electrodes, a process taking about 2+5 seconds. The amplitude is
346 automatically titrated until the threshold for repeatable foot movement, irrespective of direction, is determined.
347 This threshold amplitude is used as the base for searches in subsequent phases. In phase two (twitch response),
348 the algorithm searches for candidate stimulation sites, using twitches rather than tetanic contractions to speed-up
349 search time and reduce sensation. Four pulses of stimulation are applied to each electrode in turn. The foot
350 response is monitored for short periods after each stimulation, if there is a detectable response it is added to
351 the list of candidate sites. Again the current is automatically adjusted until between 4 and 12 sites are found or the
352 maximum current limit is reached. These sites are ranked in order of sensitivity using a cost function based on
353 the angular displacement. The first two stages therefore allowed for rapid identification of the most sensitive
354 VEs.

355 In phase three (tetanic testing), up to 8 of the sites identified in phase two were tested in rank order with an
356 increasing stimulation intensity. Stimulation began at the level identified in phase two and incremented in steps
357 until one of the following conditions were met: either [plantarflexion was corrected to neutral dorsiflexionzero
358 dorsiflexion](#); or current reaching twice the starting value; or 150% of starting value with no movement detected;
359 or motion saturation was detected. The algorithm included safeguards if unexpected movements occurred.

360 [enabling the system to temporarily wait if a leg spasm was detected or to pause the search process if repeated](#)
361 [non-stimulated leg movement was detected.](#) Once all the candidate sites were assessed, they were given a score
362 based on a three-part cost function, designed to penalise solutions resulting in plantarflexion, excessive
363 inversion or eversion, and high current [\[24\]](#) [If at any point during this phase the user found a site uncomfortable](#)
364 [the clinician was able to skip that site. Once the tetanic testing phase was complete the](#) ~~The user then stood and~~
365 ~~the first-ranked site was activated and, after initial testing of the site while sitting,~~ ~~the user then walked using~~
366 [the stimulator: If the foot response or stimulation sensation was not satisfactory it could be manually changed to](#)
367 [an alternative site if the response was not satisfactory it could be manually changed to an alternative from](#) the
368 ranking list. Finally, ~~overall~~ stimulus pulse width could be adjusted by the user, if necessary, to fine-tune the
369 magnitude of foot response.

370 [5.34.3](#) Laboratory-based clinical study

371 Ten participants with drop foot due to stroke (ages 53–71 years) and 11 due to MS (ages 40–80 years) were
372 recruited to test the system. Each participant walked twice over 10 m under each of four conditions; [a\)](#)1. using
373 their own stimulator setup by themselves; [b\)](#)2. using their own stimulator set up by a clinician, [c\)](#)3. using
374 ShefStim with automated setup, and [d\)](#)4. no stimulation. Outcome measures were walking speed, foot angle at
375 initial contact and the Borg Rating of Perceived Exertion. As described in Heller et al [\[24\]](#)[\[6\]](#), the results
376 showed that when setup using ShefStim subjects' walking speed, dorsiflexion and frontal plane ankle angle at
377 initial contact were all broadly comparable with clinician setup and, apart from walking speed, better than
378 patient setup. The study demonstrated for the first time that [fully](#) automated setup of an array stimulator is
379 feasible in a population with drop foot of central origin.

380 [65](#). FIRST TAKE-HOME STUDY OF SHEFSTIM

381 A final iteration of the stimulator design resulted in the CE- marked ShefStim system shown below.



382
383 *Figure 5: ShefStim stimulator (left) being used by a subject during setup (right)*

384

385 The ShefStim stimulator measures 142mm x 50mm x 14mm (volume 99cc) and weighs 125 g (including
386 batteries). In contrast to the earlier versions of the system, it includes a combined foot angle sensor and
387 remote control device, and setup does not involve holding the leg in a brace ([Figure 5](#)). The remote control device is
388 placed on the foot during set up and wirelessly provides triaxial accelerometer inputs to the search algorithm
389 described in the previous section. [Users are provided with an attachment, based on an iPod holder, which could](#)
390 [be slipped onto the shoe prior to setup. Guidance is provided to the users on the correct mounting of the remote](#)
391 [control on the shoe and the importance of aligning the ShefStim box with the long axis of the leg.](#) Once setup is
392 completed, the foot angle sensor device serves as a remote control with which the user can pause stimulation,
393 adjust intensity or receive audible error messages. [Stimulation timing during gait is controlled using a](#)
394 [conventional footswitch, located under the heel of the shoe.](#) Integrating the foot angle sensor into the system
395 enabled the stimulator to carry out the automated setup routine without requiring input from any external
396 sensors or connection to a PC, making it suitable for use in the home environment.

397 In the final clinical study seven subjects with drop foot (3 subjects with MS, 3 with stroke and 1 with
398 traumatic brain injury) used ShefStim over a 2 week period. The reader is referred to [\[22\]](#)[\[7\]](#) for the experimental protocol

399 and full results. Log data showed that all subjects were able to setup the stimulator outside of the laboratory
400 environment without technical support. Automated setup time ~~_~~ averaged 9 minutes, plus 5 minutes to don the
401 equipment. Despite the challenges associated with unsupervised use, including the need for users to correctly
402 align the ShefStim, placed in a pocket of a leg-mounted sleeve, and the remote on their shoe, Speed and foot
403 response with ~~and without~~ ShefStim, ~~were~~ evaluated in a gait laboratory at the end of the 2 week period ~~and~~
404 showed results ~~were~~ comparable with the previous study by Heller [21][6]. ~~In addition,~~ The study
405 demonstrated, for the first time, that array-based automated setup FES system for foot-drop can be successfully
406 used without technical support outside of the laboratory environment.

407 7.6. DISCUSSION AND CONCLUSIONS

408 The work presented in this paper describes the evolution of the ShefStim design from initial concept in 2003 to
409 evaluation of the CE-marked system by people with stroke in their own homes. A number of issues are worth
410 discussing before conclusions are drawn on the revisions needed to be made to the design.

411 In section 2 we introduced two models used for the identification of electrode array geometry. The activation
412 area is similar in concept to the measure used by Kuhn et al [29], who based their measure of selectivity on an
413 activation volume. As our model assumes the nerve depth to be known (at 10mm in this case), the cross-
414 sectional area of the stimulation pool at 10mm is the measure of the selectivity of stimulation. The larger this
415 area is, the less selective the array stimulation is (i.e. the worse the ability to selectively stimulate neural
416 structures). ~~There are a number of limitations with the model, including the prismatic geometry and~~
417 ~~assumptions regarding the nerve depth, which undoubtedly varies significantly between subjects. Further, in~~
418 ~~contrast to Kuhn et al. [29], we did not experimentally validate the model. However, the array geometry and~~
419 ~~hydrogel properties derived using the model proved to be similar to the array design successfully used in the~~
420 ~~final take-home study. Our model was not as detailed as the Kuhn model; for example, the model geometry was~~
421 ~~a greatly simplified representation of the true anatomy, and we did not investigate the effects of modelled nerve~~
422 ~~depth on selectivity.~~

423

424 Although the ShefStim stimulator has been CE marked, there remain a small number of barriers to clinical
425 uptake. By far the most significant of these is that sweat ingress to the hydrogel electrode interface layer leads to
426 a significant drop in its resistivity and an inevitable decay in focality and stimulation efficiency with wear time
427 [23][30]. These effects limit use of a given array to around one day of continuous wear. In the final study of
428 ShefStim [22][7] we were able to provide participants with sufficient arrays to use a fresh hydrogel layer each
429 day. However, the cost of such an approach is high and not a realistic solution in clinical practice. To address
430 this we are exploring alternative solutions, including the use of dry electrodes (see, for example [24][31]). Other
431 minor product development issues remain, including the development of an improved garment to house the
432 stimulator on the leg and minor improvements to the firmware, all of which may be easily resolved. We believe
433 that these improvements would lead to a significant reduction in setup time, as recorded in our final
434 (unsupervised) study [7].

435 In conclusion, this paper has described the complete design, development and evaluation of an array-based FES
436 system with automated setup for the correction of drop foot. The results demonstrate that an array-based
437 stimulator with automated setup is a viable alternative to a conventional surface stimulator, or an implanted
438 stimulator, for the correction of drop foot. Longer term clinical exploitation of ShefStim is dependent on
439 identifying an acceptable alternative to the high-resistivity hydrogel electrode-skin interface layer.

440 Acknowledgements

441 This is a summary of independent research funded by the National Institute for Health Research (NIHR) under
442 its Invention for Innovation (i4i) Programme (grant ref HTD480), UK Overseas Research Studentship and
443 Sheffield Hospitals Charitable Trust. The views expressed are those of the author(s) and not necessarily those of
444 the NHS, the NIHR or the Department of Health, or other funding bodies.

445

446

447 [1] NICE. Functional electrical stimulation for drop foot of central neurological origin (interventional
448 procedures overview) 2008.

449 [2] Taylor PN, Burridge JH, Dunkerley AL, Lamb A, Wood DE, Norton JA, et al. Patients' perceptions of the
450 Odstock Dropped Foot Stimulator (ODFS). Clin Rehabil. 1999;13:439-46.

451 [3] Heller BW, Clarke AJ, Good TR, Healey TJ, Nair S, Pratt EJ, et al. Automated setup of functional electrical
452 stimulation for drop foot using a novel 64 channel prototype stimulator and electrode array: results from a gait-
453 lab based study. Med Eng Phys. 2013;35:74-81.

454 [4] Prenton S, Kenney LP, Stapleton C, Cooper G, Reeves ML, Heller BW, et al. Feasibility study of a take-
455 home array based functional electrical stimulation system with automated setup for current functional electrical
456 stimulation users with foot drop. *Arch Phys Med Rehabil.* 2014;95:1870-7.
457 [5] Burridge JH, Haugland M, Larsen B, Pickering RM, Svaneborg N, Iversen HK, Christensen PB, Haase J,
458 Brennum J, Sinkjaer T. Phase II trial to evaluate the ActiGait implanted drop foot stimulator in established
459 hemiplegia. *J Rehabil Med.* 2007;39:212-8.
460 [6] Kottink AI, Hermens HJ, Nene AV, Tenniglo MJ, van der AaHE, Buschman HP, Ijzerman MJ. A
461 randomized controlled trial of an implantable 2 channel peroneal nerve stimulator on walking speed and activity
462 in poststroke hemiplegia. *Arch Phys Med Rehabil.* 2007;88:971-8.
463 [7] Merson E, Swain I, Taylor P, Cobb J. Two channel stimulation for the correction of drop foot. 5th
464 Conference of IFESS UK & Ireland. Sheffield, UK, 2015.
465 [8] Seel T, Valtin M, Werner C, Schauer T. Multivariable Control of Foot Motion During Gait by Peroneal
466 Nerve Stimulation via two Skin Electrodes. 9th IFAC Symposium on Biological and Medical Systems. Berlin,
467 Germany, 2015.
468 [9] Whitlock T, Peasgood W, Fry M, Bateman A, Jones R. Self-optimising electrode arrays. 5th IPEM—Clinical
469 Functional Electrical Stimulation Meeting. Salisbury 1997.
470 [10] Elsaify E, Fothergill J, Peasgood W. A portable FES system incorporating an electrode array and feedback
471 sensors. 8th Vienna International workshop functional electrical stimulation. Vienna, Austria 2004.
472 [11] Hernandez JD. Development and Evaluation of a Surface Array Based System to Assist Electrode
473 Positioning in FES for Drop Foot: University of Surrey; 2009.
474 [12] Kuhn A, Keller T, Micera S, Morari M. Array electrode design for transeutaneous electrical stimulation: a
475 simulation study. *Med Eng Phys.* 2009;31:945-51.
476 [13] Kenney L, Heller B, Barker AT, Reeves M, Healey J, Good T, et al. The Design, Development and
477 Evaluation of an Array Based FES System with Automated Setup for the Correction of Drop Foot. 9th IFAC
478 Symposium on Biological and Medical System. Berlin, Germany 2015.
479 [14] Heller B, Barker AT, Sha N, Newman J, Harron E. Improved control of ankle movement using an array of
480 mini electrodes. FES User Day Conference. Birmingham, U.K. 2003.
481 [15] Sha N, Heller BW, Barker AT. 3D modelling of a hydrogel sheet—electrode array combination for surface
482 functional electrical stimulation. Proceedings of the 9th Annual Conference of IFESS. Bournemouth, UK 2004.
483 p. 431-35
484 [16] Rattay F. Analysis of models for external stimulation of axons. *IEEE Trans Biomed Eng.* 1986;33:974-7.
485 [17] Sha N. A surface electrode array based system for functional electrical stimulation: University of Salford;
486 2009.
487 [18] Sha N, Kenney LP, Heller BW, Barker AT, Howard D, Wang W. The effect of the impedance of a thin
488 hydrogel electrode on sensation during functional electrical stimulation.
489 *Med Eng Phys.* 2008;30:739-46.
490 [19] Sha N, Kenney LP, Heller BW, Barker AT, Howard D, Moatamedi M. A finite element model to identify
491 electrode influence on current distribution in the skin. *Artif Organs.* 2008;32:639-43
492 [20] Woodburn J, Helliwell PS, Barker S. Three dimensional kinematics at the ankle joint complex in
493 rheumatoid arthritis patients with painful valgus deformity of the rearfoot. *Rheumatology (Oxford).*
494 2002;41:1406-12.
495 [21] Heller BW, Clarke AJ, Good TR, Healey TJ, Nair S, Pratt EJ, Reeves ML, van der Meulen JM, Barker AT.
496 Automated setup of functional electrical stimulation for drop foot using a novel 64 channel prototype stimulator
497 and electrode array: results from a gait lab based study. *Med Eng Phys.* 2013;35:74-81
498 [22] Prenton S, Kenney LP, Stapleton C, Cooper G, Reeves ML, Heller BW, Sobuh M, Barker AT, Healey J,
499 Good TR, Thies SB, Howard D, Williamson T. Feasibility study of a take-home array based functional
500 electrical stimulation system with automated setup for current functional electrical stimulation users with
501 foot drop. *Arch Phys Med Rehabil.* 2014;95:1870-7.
502 [23] Cooper G, Barker AT, Heller BW, Good T, Kenney LP, Howard D. The use of hydrogel as an electrode-
503 skin interface for electrode array FES applications. *Med Eng Phys.* 2011;33:967-72.
504 [24] Yang K, Freeman C, Torah R, Beeby S, Tudor J. Screen printed fabric electrode array for wearable
505 functional electrical stimulation. *Sensor Actuat a Phys.* 2014;213:108-15.
506
507 [1] NICE. Functional electrical stimulation for drop foot of central neurological origin.
508 National Institute for Clinical Excellence; 2009. p. 2.
509 [2] Bosch PR, Harris JE, Wing K, American Congress of Rehabilitation Medicine Stroke
510 Movement Interventions S. Review of therapeutic electrical stimulation for dorsiflexion assist
511 and orthotic substitution from the American Congress of Rehabilitation Medicine stroke
512 movement interventions subcommittee. *Arch Phys Med Rehabil.* 2014;95:390-6.

- 513 [3] Roche A, Laighin G, Coote S. Surface-applied functional electrical stimulation for
514 orthotic and therapeutic treatment of drop-foot after stroke -- a systematic review. *Physical*
515 *Therapy Reviews*. 2009;14:63-80.
- 516 [4] Taylor PN, Burridge JH, Dunkerley AL, Lamb A, Wood DE, Norton JA, et al. Patients'
517 perceptions of the Odstock Dropped Foot Stimulator (ODFS). *ClinRehabil*. 1999;13:439-46.
- 518 [5] Melo PL, Silva MT, Martins JM, Newman DJ. Technical developments of functional
519 electrical stimulation to correct drop foot: sensing, actuation and control strategies. *Clin*
520 *Biomech (Bristol, Avon)*. 2015;30:101-13.
- 521 [6] Heller BW, Clarke AJ, Good TR, Healey TJ, Nair S, Pratt EJ, et al. Automated setup of
522 functional electrical stimulation for drop foot using a novel 64 channel prototype stimulator
523 and electrode array: results from a gait-lab based study. *Med Eng Phys*. 2013;35:74-81.
- 524 [7] Prenton S, Kenney LP, Stapleton C, Cooper G, Reeves ML, Heller BW, et al. Feasibility
525 study of a take-home array-based functional electrical stimulation system with automated
526 setup for current functional electrical stimulation users with foot-drop. *Arch Phys Med*
527 *Rehabil*. 2014;95:1870-7.
- 528 [8] Burridge JH, Haugland M, Larsen B, Pickering RM, Svaneborg N, Iversen HK, et al.
529 Phase II trial to evaluate the ActiGait implanted drop-foot stimulator in established
530 hemiplegia. *J Rehabil Med*. 2007;39:212-8.
- 531 [9] Kottink AI, Hermens HJ, Nene AV, Tenniglo MJ, van der Aa HE, Buschman HP, et al. A
532 randomized controlled trial of an implantable 2-channel peroneal nerve stimulator on walking
533 speed and activity in poststroke hemiplegia. *Arch Phys Med Rehabil*. 2007;88:971-8.
- 534 [10] Merson E, Swain I, Taylor P, Cobb J. Two-channel stimulation for the correction of drop
535 foot. 5th Conference of IFESS UK & Ireland. Sheffield, UK2015.
- 536 [11] Seel T, Werner C, Raisch J, Schauer T. Iterative learning control of a drop foot
537 neuroprosthesis - Generating physiological foot motion in paretic gait by automatic feedback
538 control. *Control Eng Pract*. 2016;48:87-97.
- 539 [12] Seel T, Valtin M, Werner C, Schauer T. Multivariable Control of Foot Motion During
540 Gait by Peroneal Nerve Stimulation via two Skin Electrodes. 9th IFAC Symposium on
541 Biological and Medical Systems. Berlin, Germany2015.
- 542 [13] Whitlock T, Peasgood W, Fry M, Bateman A, Jones R. Self-optimising electrode arrays.
543 5th IPEM Clinical Functional Electrical Stimulation Meeting. Salisbury1997.
- 544 [14] Elsaify E, Fothergill J, Peasgood W. A portable FES system incorporating an electrode
545 array and feedback sensors. 8th Vienna International workshop functional electrical
546 stimulation. Vienna, Austria2004.
- 547 [15] Hernandez JD. Development and Evaluation of a Surface Array Based System to Assist
548 Electrode Positioning in FES for Drop Foot: University of Surrey; 2009.
- 549 [16] Kuhn A, Keller T, Micera S, Morari M. Array electrode design for transcutaneous
550 electrical stimulation: a simulation study. *Med Eng Phys*. 2009;31:945-51.
- 551 [17] Valtin M, Steel T, Raisch J, Schauer T. Iterative learning control of drop foot stimulation
552 with array electrodes for selective activation. 19th World Congress IFAC. Cape Town, South
553 Africa2014.
- 554 [18] Hernandez MD. Development and evaluation of a surface array based system to assist
555 electrode positioning in FES for drop foot: University of Surrey; 2009.
- 556 [19] Kenney L, Heller B, Barker AT, Reeves M, Healey J, Good T, et al. The Design,
557 Development and Evaluation of an Array-Based FES System with Automated Setup for the
558 Correction of Drop Foot. 9th IFAC Symposium on Biological and Medical System. Berlin,
559 Germany2015.
- 560 [20] Heller B, Barker AT, Sha N, Newman J, Harron E. Improved control of ankle movement
561 using an array of mini-electrodes. FES User Day Conference. Birmingham, U.K.2003.

562 [21] Sha N, Heller BW, Barker AT. 3D modelling of a hydrogel sheet - electrode array
563 combination for surface functional electrical stimulation. Proceedings of the 9th Annual
564 Conference of IFESS. Bournemouth, UK2004. p. 431-3.
565 [22] Duck FA. Physical properties of tissue : a comprehensive reference book. London:
566 Academic Press; 1990.
567 [23] Rattay F. Analysis of models for external stimulation of axons. IEEE Trans Biomed Eng.
568 1986;33:974-7.
569 [24] Sha N. Development of a steerable electrode array for functional electrical stimulation:
570 Sheffield University; 2003.
571 [25] Sha N, Kenney LP, Heller BW, Barker AT, Howard D, Wang W. The effect of the
572 impedance of a thin hydrogel electrode on sensation during functional electrical stimulation.
573 Med Eng Phys. 2008;30:739-46.
574 [26] Sha N, Kenney LP, Heller BW, Barker AT, Howard D, Moatamedi M. A finite element
575 model to identify electrode influence on current distribution in the skin. Artif Organs.
576 2008;32:639-43.
577 [27] Sha N. A surface electrode array-based system for functional electrical stimulation:
578 University of Salford; 2009.
579 [28] Woodburn J, Helliwell PS, Barker S. Three-dimensional kinematics at the ankle joint
580 complex in rheumatoid arthritis patients with painful valgus deformity of the rearfoot.
581 Rheumatology (Oxford, England). 2002;41:1406-12.
582 [29] Kuhn A, Keller T, Lawrence M, Morari M. The influence of electrode size on selectivity
583 and comfort in transcutaneous electrical stimulation of the forearm. IEEE Trans Neural Syst
584 Rehabil Eng. 2010;18:255-62.
585 [30] Cooper G, Barker AT, Heller BW, Good T, Kenney LP, Howard D. The use of hydrogel
586 as an electrode-skin interface for electrode array FES applications. Med Eng Phys.
587 2011;33:967-72.
588 [31] Yang K, Freeman C, Torah R, Beeby S, Tudor J. Screen printed fabric electrode array
589 for wearable functional electrical stimulation. Sensor Actuat a-Phys. 2014;213:108-15.
590